FINAL REPORT

DYNAMIC ANALYSIS OF GAS-CORE REACTOR SYSTEM

STAR

SCIENCE, TECHNOLOGY AND RESEARCH, INC.

SUITE 460 1100 SPRING ST., NW
ATLANTA, GEORGIA 30309

FINAL REPORT

DYNAMIC ANALYSIS OF GAS-CORE REACTOR SYSTEM

BY

SCIENCE, TECHNOLOGY AND RESEARCH, INC.
SUITE 460
1100 SPRING STREET
ATLANTA, GEORGIA 30309

PREPARED FOR

NATIONAL AERONAUTICS AND SPACE ADMINISTRATION

MARCH 1973
CONTRACT NAS3-16735

NASA LEWIS RESEARCH CENTER
CLEVELAND, OHIO 44135

PROJECT MANAGER - STAR
KYLE H. TURNER, JR.

CONTRACT MONITOR - NASA
ALBERT F. KASCAK

TABLE OF CONTENTS

LIST OF FIGURES

ABSTRACT

A NASA-supplied heat transfer analysis was incorporated into a previously developed model CØDYN to obtain a model of open-cycle gaseous core reactor dynamics which can predict the heat flux at the cavity wall. The resulting model was used to study the sensitivity of the model to the value of the reactivity coefficients and to determine the system response for twenty specified perturbations. In addition, the model was used to study the effectiveness of several control systems in controlling the reactor. It was concluded that control drums located in the moderator region capable of inserting reactivity quickly provided the best control.

Section 1

SUMMARY

A NASA-supplied heat transfer analysis was incorporated into a previously developed model of open cycle gas-core dynamics (CØDYN). The resulting model was capable of calculating the heat flux at the cavity wall as a function of time. The model was used to study the model's sensitivity to variations in the reactivity coefficients and to determine the predicted response for twenty specified perturbations. In addition, the model was used to study the effectiveness of several control systems in controlling the reactor.

It was found that the model is sensitive to variations in propellant temperature, propellant density and fuel cloud expansion coefficients of reactivity. The model is also sensitive to large changes in the fuel temperature coefficient. Variations in the fuel mass and moderator temperature coefficients had virtually no effect on the model.

The responses obtained for all reactivity insertions were qualitatively the same; the power behaved in oscillatory fashion with the oscillations superimposed on smaller changes in the average power. The smaller changes were toward higher power levels for positive insertions and lower levels for negative insertions. Larger insertions produced larger oscillations. For positive insertions, the larger the inserted reactivity, the sooner the reactor reached conditions which could be dangerous. For a positive reactivity insertion of .65%, the wall heat flux reached burnout at .75 seconds and the cavity pressure reached 110% of its design value by .3 seconds.

Decreasing the rate of propellant injection causes a fairly rapid rise in reactor power. The response is again oscillatory, but the rise in average power is much more dramatic. For a 20% decrease in the propellant inlet flow rate, cavity pressure was 10% above design level by 2.3 seconds, and the wall burnout condition was reached almost

instantaneously. Increasing the propellant injection rate caused the opposite results; the reactor was essentially shut down.

Variations in the fuel injection rate had negligible effect on the state of the reactor.

Control systems using reactor power, propellant temperature and cavity pressure as the monitored parameters and reactivity, propellant injection rate and fuel injection rate as the controlled parameters were investigated. Fuel injection control was found to be inadequate in controlling perturbations of interest. Propellant injection control was found to be considerably dangerous when used with an automatic control system because several situations caused wall burnout in attempts to control the reactor. Reactivity control, probably through the use of poison drums in the moderator region was found to be the best candidate for reactor control, although the delay time for direct linear control must be on the order of 10^{-3} seconds. The three monitored parameters served equally well as measure of the reactor's control needs.

Section 2
INTRODUCTION

The gaseous core nuclear reactor was originally conceived in the process of searching for a better means of rocket propulsion for long range space missions. The two parameters of primary importance in evaluating the suitability of a given propulsion system are the specific impulse and the thrust-to-weight ratio.[1] Today's chemical rockets produce a specific impulse of about 500 seconds, and the solid core nuclear rocket is expected to eventually yield an I_{sp} of 1000 sec.[2] In designs currently being studied, the gaseous-core nuclear rocket is expected to produce an I_{sp} of 5000 sec.[3]

The gaseous core nuclear reactor is based on the concept of a fissioning uranium plasma transferring heat radiatively to a hot gas which serves as the working fluid. Two types of gas-core reactors are currently under study; they are (1) the closed cycle or nuclear light bulb and (2) the coaxial flow reactor. The nuclear light bulb concept involves containing the uranium plasma by a thin transparent wall through which the thermal radiation passes to heat the working fluid. The coaxial-flow reactor utilizes a slow moving central stream of gaseous fissioning fuel to radiatively heat a more rapidly moving annular stream of particle-seeded gas which serves as the working fluid. The original work on the coaxial flow reactor was performed by Rom[4] (who obtained a patent) and Ragsdale[5,6] and they have directed extensive studies of this concept over the past 10 years. McLafferty[7] obtained the first patent on the nuclear light bulb concept which has been examined also during the past decade.[8,9]

Recently, the increasing concern over thermal and other forms of environmental pollution has led to the search for more efficient terrestrial power generation systems. Magnetohydrodynamic (MHD) generation has shown some promise, but there has been a lack of suitable heat sources. The gaseous core reactor seems to fill this gap perfectly. In fact, Rosa states that the gas core reactor may very well prevent MHD technology from becoming obsolete.[10] Several design studies of gas-core MHD power plants and propulsion systems have been reported.[10-14] One study[14] concluded that

large commercial power plants using a gas core reactor might have thermal efficiencies as high as 75 percent. Other advantages include very high fuel economy and the reduction of thermal pollution per electrical megawatt by a factor of three to five over today's plants.

In addition to these applications, a gaseous core form of the fast breeder reactor has been proposed.[15] This study, by Kallfelz and Williams, used a one-dimensional diffusion theory code to study the effects on criticality and breeding ratio of various fuel and blanket radii.

The operation of the coaxial flow gaseous core nuclear rocket engine which is studied in this research can be described as follows: Uranium fuel is fed into the reactor cavity in solid form where it is vaporized and contained by a faster-moving stream of hydrogen propellant gas flowing coaxially around the central fuel cloud. The walls of the cavity are made of a porous material so that the propellant may be introduced uniformly over the inner surface, thus providing better fuel containment and helping to limit the wall temperature to a reasonable value. The propellant is heated by thermal radiation from the fissioning fuel cloud and is expelled through the exhaust nozzle producing the engine thrust. Since the propellant at its cavity entrance temperature is essentially transparent to the radiation being emitted from the fuel cloud, the hydrogen must be seeded with small particles which render the mixture entering the cavity opaque to radiant energy and thereby prevent any significant heat flux from reaching the cavity walls. That fraction of the energy produced in the fuel which is not emitted as thermal radiation is released in the form of gamma rays and neutrons which deposit heat in the moderator. The moderator rejects heat to the helium primary coolant which, in turn, rejects heat to the space radiator and turbine circuits via the primary heat exchanger. Most of the energy deposited in the moderator by gamma ray absorption and neutron slowing down is conveyed to the space radiator where it is dumped into space; the remainder of the heat is used to operate a turbine and generate power. The fuel is fully enriched uranium 235, the propellant is hydrogen seeded with tungsten (0.2% by weight), and the moderator is beryllium oxide. Both secondary working fluids are liquid sodium.

Robert G. Ragsdale and his co-workers at the NASA Lewis Research Center have determined most of the nominal steady state operating conditions for the system. These conditions are listed in Table 2-1.

Table 2-1. Nominal Steady State Operating Conditions for the Coaxial Flow Gaseous Core Reactor

Reactor Power	5900 megawatts
Fuel Temperature (avg)	90,000°R
Propellant Temperature (avg)	19,100°R
Cavity Pressure	350 atmospheres
Fuel Exit Flow Rate	.1 pounds/sec
Propellant Exit Flow Rate	10 pounds/sec
Fuel Mass	100 kilograms
Fuel Radius	4.66 feet
Cavity Radius	7 feet
Propellant Density	.026 pounds/ft^3
Moderator Temperature	1600°R

Section 3

DERIVATION OF THE MODEL

The primary objective of the first task was the inclusion of a heat transfer analysis, which provides the ability to calculate the heat flux at the cavity wall, and a pump equation, which gives the propellant injection rate as a function of cavity pressure, in the previously developed open-cycle gas-core dynamics model CØDYN. Both the heat transfer analysis and the pump equation were supplied by NASA. The derivation of the CØDYN equation set is thoroughly described in Reference 16. For the purposes of this study, the equations describing the moderator cooling system were replaced by an equation predicting essentially constant heat removal from the moderator; an exact representation of each cooling system component does not affect the model's predictions but does require large amounts of computer time.

Heat Transfer Analysis

The heat transfer analysis was supplied by Albert F. Kascak of the NASA-Lewis Research Center. The following discussion is not intended to be a thorough analysis of the dynamic heat transfer processes of the gas core reactor, but it is presented here to familiarize the reader with the techniques used to obtain the results described later in this report. The entire discussion is taken from an informal technical note received by STAR from Mr. Kascak in June of 1972. Understanding of the following development will be enhanced by study of the list of symbols appearing in Table 3-1.

The discussion will be begun by examining the heat transfer processes at steady state conditions. First, let h and p be the variables of state; thus,

Table 3-1. List of Symbols Used in the Heat Transfer Discussion

	Symbols
p	cavity pressure
h	enthalpy
q	heat flux
ρ	density
v	propellant velocity
C_p	specific heat
k_{th}	thermal conductivity
a_R	absorption coefficient
σ	Stefan-Boltzmann constant
x	distance from fuel surface towards cavity wall
T	temperature
t	time
ρv	propellant injection rate per unit area
	Subscripts
o	at fuel-propellant interface ($x = 0$)
∞	at large x
BO	at wall burnout heat flux
x	at the cavity wall
	Superscripts
*	reference
max	maximum heat flux at fuel surface for wall burnout

$$
\begin{aligned}
C_p &= C_p(h,p) \\
\rho &= \rho(h,p) \\
a_R &= a_R(h,p) \\
k_{th} &= k_{th}(h,p) \\
T &= T(h,p)
\end{aligned}
\tag{3-1}
$$

Now, define the total heat conductivity of the propellant, K, by

$$K = \frac{16\sigma T^3}{3a_R} \tag{3-2}$$

At steady state, the energy equation is given by

$$\rho v \frac{dh}{dx} = \frac{dq}{dx} \tag{3-3}$$

If, as is common when discussing heat transfer in the core of a gaseous core reactor, the conduction approximation of radiant heat transfer is used, one may write

$$q = -K \frac{dT}{dx} \tag{3-4}$$

Now, if ρv is assumed constant, equation (3-3) may be solved to yield

$$q = \rho v \, (h - h_\infty) \tag{3-5}$$

Thus,

$$-K \frac{dT}{dx} = \rho v \, (h - h_\infty) \tag{3-6}$$

Or, since $\frac{dT}{dx} = \frac{1}{C_p} \frac{dh}{dx}$,

$$\frac{-K}{C_p} \frac{dh}{dx} = \rho v (h - h_\infty) \tag{3-7}$$

Rearrangement of (3-7) gives

$$\frac{dx}{dh} = \frac{-K}{C_p (h - h_\infty) \rho v} \tag{3-8}$$

Defining

$$g(h,p) = \frac{-K}{C_p(h - h_\infty)} \tag{3-9}$$

and

$$G(h,p) = \int_h^{h^*} g \, dh \tag{3-10}$$

one may write from (3-8)

$$\frac{dx}{dh} = -g/\rho v \tag{3-11}$$

integration then results in

$$x = \frac{1}{\rho v} \left(G(h,p) - G(h_o,p) \right) \tag{3-12}$$

It should be noted that all the above equations hold for all x between the fuel-propellant interface and the cavity wall, i.e., $x_o < x < x_w$.

Armed with these results, the discussion can move into the transient analysis as follows. The time-dependent energy equation is written as

$$\frac{d(\rho h)}{dt} + \frac{d(\rho v h)}{dx} = - \frac{dq}{dx} \tag{3-13}$$

Integration of (3-13) yields (assuming $q_\infty = 0$)

$$\int_0^\infty \frac{d(\rho h)}{dt} \, dx = -q_o + \rho v (h_o - h_\infty) \tag{3-14}$$

Now, let $\frac{d(\rho h)}{dt} = 0$ for $x > x_w$; the left-hand term of equation (3-14) then becomes

$$\int_0^\infty \frac{d(\rho h)}{dt} \, dx = \frac{d}{dt} \int_0^{x_w} \rho h \, dx = \frac{d}{dt} \int_{h_o}^{h_w} h \frac{dx}{dh} \, dh \tag{3-15}$$

Assume, now, that $\frac{dx}{dh}$ is equal to its steady state value as given by equation (3-11). One may then write (by combining the results of (3-11) and (3-15))

$$\int_0^\infty \frac{d(\rho h)}{dt} \, dx = \frac{d}{dt} \int_{h_o}^{h_w} - \frac{\rho h g}{\rho v} \, dh \tag{3-16}$$

If f and F are defined by

$$f(h,p) = \rho h g \tag{3-17}$$

and

$$F(h,p) = \int_{h}^{h^*} f \, dh \tag{3-18}$$

equation (3-16) becomes

$$\int_0^\infty \frac{d(\rho h)}{dt} \, dx = \frac{d}{dt} \left(\frac{1}{\rho v} \left(F(h_w,p) - F(h_o,p) \right) \right) \tag{3-19}$$

Expanding the differential of equation (3-19) gives

$$\int_0^\infty \frac{d(\rho h)}{dt} \, dx = -\frac{1}{(\rho v)^2} (F_w - F_o) \frac{d(\rho v)}{dt} + \frac{1}{\rho v} \left(\frac{dF_w}{dt} - \frac{dF_o}{dt} \right) \frac{dp}{dt}$$

$$+ \frac{1}{\rho v} \left(f_o \frac{dh_w}{dt} - f_w \frac{dh_w}{dt} \right) \tag{3-20}$$

In practice, it is found that F is not dependent on the cavity pressure p and that $\frac{dh_w}{dt}$ is zero; deleting the terms containing $\frac{dF}{dt}$ and $\frac{dh_w}{dt}$ from equation (3-20), substituting the result in equation (3-14), and solving for $\frac{dh_o}{dt}$ yields

$$\frac{dh_o}{dt} = \frac{\rho v}{f_o} \left(\frac{(F_w - F_o)}{(\rho v)^2} \frac{d(\rho v)}{dt} - q_o + v(h_o - h) \right) \tag{3-21}$$

which is the basic dynamic equation from which all the heat transfer calculations are made.

Once h_o is known at time t, h_w may be found from a knowledge of the function G by the use of equation (3-12) with $x=x_w$. The wall heat flux may then be found from a knowledge of the enthalpy versus temperature curve for hydrogen.

The value of ρv at $t = 0$ (steady state) is found as follows.

At wall burnout conditions, equation (3-12) is written as

$$x_w = \frac{1}{\rho v} \left(G(h_{BO},p) - G(h_\infty + q_o^{max}/\rho v \ , \ p)\right) \qquad (3\text{-}22)$$

all parameters in equation (3-22) except ρv are known. Since (3-22) is transcendental inρv, a Newton-Raphson iterative root-finding subprogram called NEWTIT is used to find the initial value of ρv. It should be noted that in this analysis it is assumed that the reactor in steady state is operating at about 90% below wall burnout, i.e., that $q_o = \eta q_o^{max}$ where $\eta = .1$. Since (rearranging equation (3-5) with $h \approx h_o$)

$$h_o = h_\infty + \eta q_o^{max}/\rho v \qquad (3\text{-}23)$$

the value of ρv found from equation (3-22) corresponds to the propellant injection rate required to operate the reactor at 90% below wall burnout. For times after $t = 0$, ρv was taken to be $\varepsilon \dot{m}_{p_i}$ and $\frac{d(\rho v)}{dt}$ to be $\varepsilon \frac{d\dot{m}_{p_i}}{dt}$ where

$$\varepsilon = \rho v / \dot{m}_{p_i} \Big|_{t=0} \qquad (3\text{-}24)$$

The functions G and F were evaluated at various temperatures and pressures through the use of the subroutine PRØPER which was also supplied by Mr. Kascak.

Pump Equation

The pump equation supplied by the contract monitor which best describes the flow characteristics of the pump expected to be used in the gas core reactor is:

$$\dot{m}_{p_i} = .0000625 \ p \qquad (3\text{-}25)$$

Section 4

SENSITIVITY OF THE MODEL TO REACTIVITY COEFFICIENTS

The objective of Task II was to determine the sensitivity of the model to variations in the reactivity coefficients. NASA has supplied reference values for the coefficients, and the possible uncertainty in those values was indicated by giving upper and lower limits for the range in which the values are expected to lie. The reference values and the range of uncertainty for each coefficient are listed in Table 4-1.

Table 4-1. Reactivity Coefficients and Their Range of Uncertainty

Coefficient	Reference Value	Upper Limit	Lower Limit
Fuel Mass	.26	.31	.21
Fuel Temperature	.001	.002	-.5
Fuel Radius	.21	.3	.15
Propellant Density	-.19	-.1	-.2
Propellant Temperature	-.2	-.05	-.5
Moderator Temperature	-.018	-.009	-.025

Task II was completed as follows. First, a single run was made with CØDYN II to determine the system response to a step insertion of .65% (one dollar) reactivity. Then, to find the model's sensitivity to variations in reactivity coefficients, twelve response predictions were made; in each run, one of the reactivity coefficients was set equal to the upper or lower bound as indicated in Table 4-1. The perturbation for all of the sensitivity runs was a positive step insertion of .65% reactivity, and the sensitivity was determined by comparing

each of these twelve runs to the results obtained using the reference coefficients.

The predicted response for a positive step insertion of .65% reactivity using the reference coefficients is shown in Figure 4-1. The power response can best be described as a damped oscillation superimposed upon a slow, steady rise in average power. The initial power peak is about 60% above design power and occurs about 200 milliseconds after the insertion. The other parameters describing the state of the reactor (cavity pressure, fuel and propellant temperatures, flow rates, etc.) oscillate also, but their deviations from the design values are somewhat smaller than that observed in the power response. These oscillations are phase-shifted by about 200 milliseconds with respect to the power curve. Cavity pressure first reaches 110% of design level at about 300 milliseconds after the perturbation but does not exceed 115% of steady state in the five-second time period for which the response was calculated. The cavity wall heat flux first exceeds burnout at about 0.75 seconds; the second occurance comes at about 1.5 seconds. In the first instance, burnout conditions last 250 milliseconds, but the wall heat flux does not drop below the burnout value after 1.5 seconds.

The generation of the characteristic response can be analyzed through the reactivity plots of Figure 4-2. Concurrent increases in propellant temperature and density provide sufficient negative feedback to more than offset a positive reactivity contribution due to fuel cloud expansion. The net result is that the total reactivity decreases and the power level drops. With the drop in power come corresponding reversals in the behavior of the three parameters mentioned above; the negative propellant temperature contribution decreases, the negative propellant density contrubition decreases and actually becomes positive, and the positive fuel expansion contribution decreases. The total negative reactivity introduced by the trend reversals is, however, less than the original insertion,

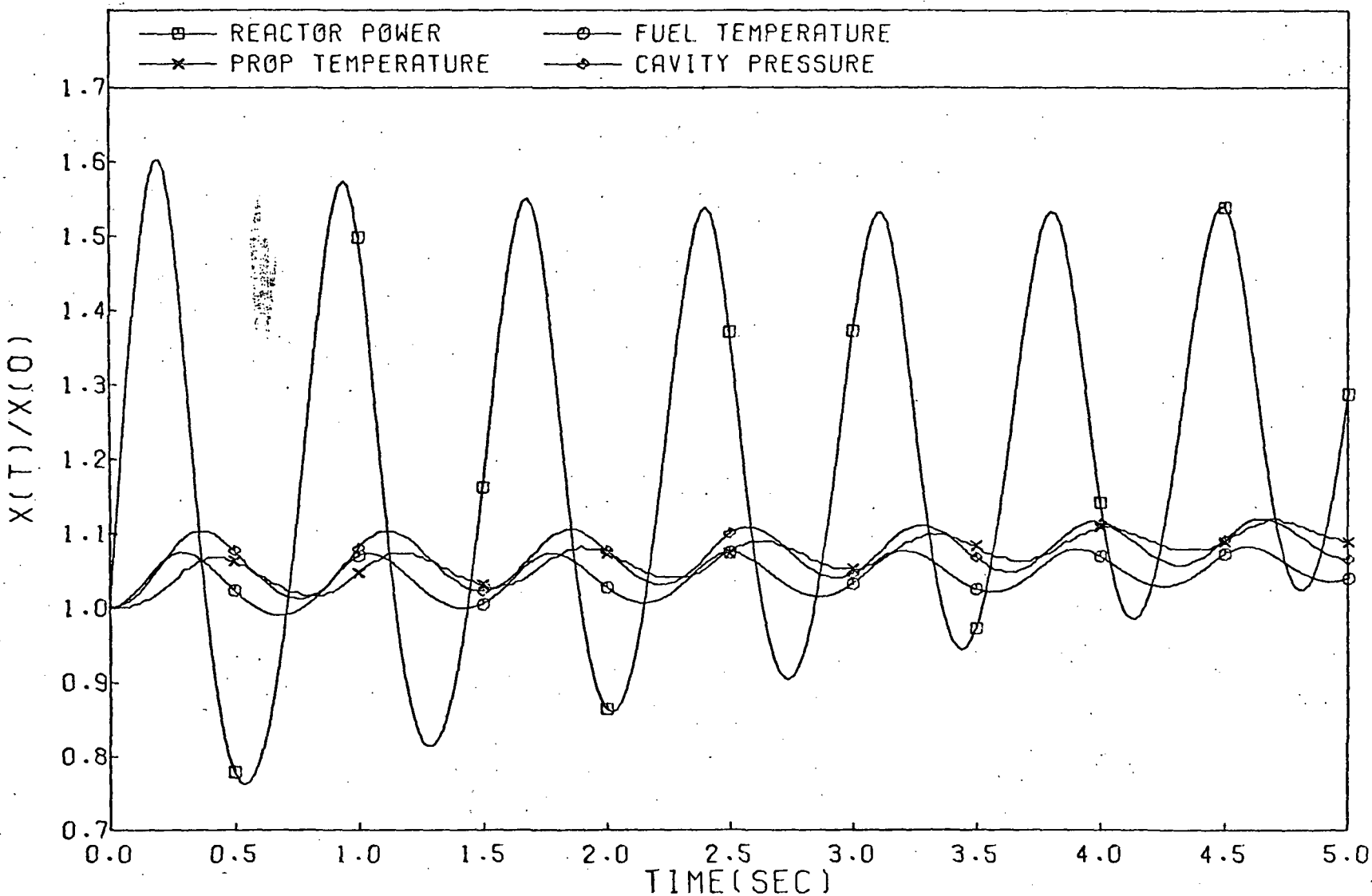

Figure 4-1. Response for Step Insertion of +0.65% Reactivity

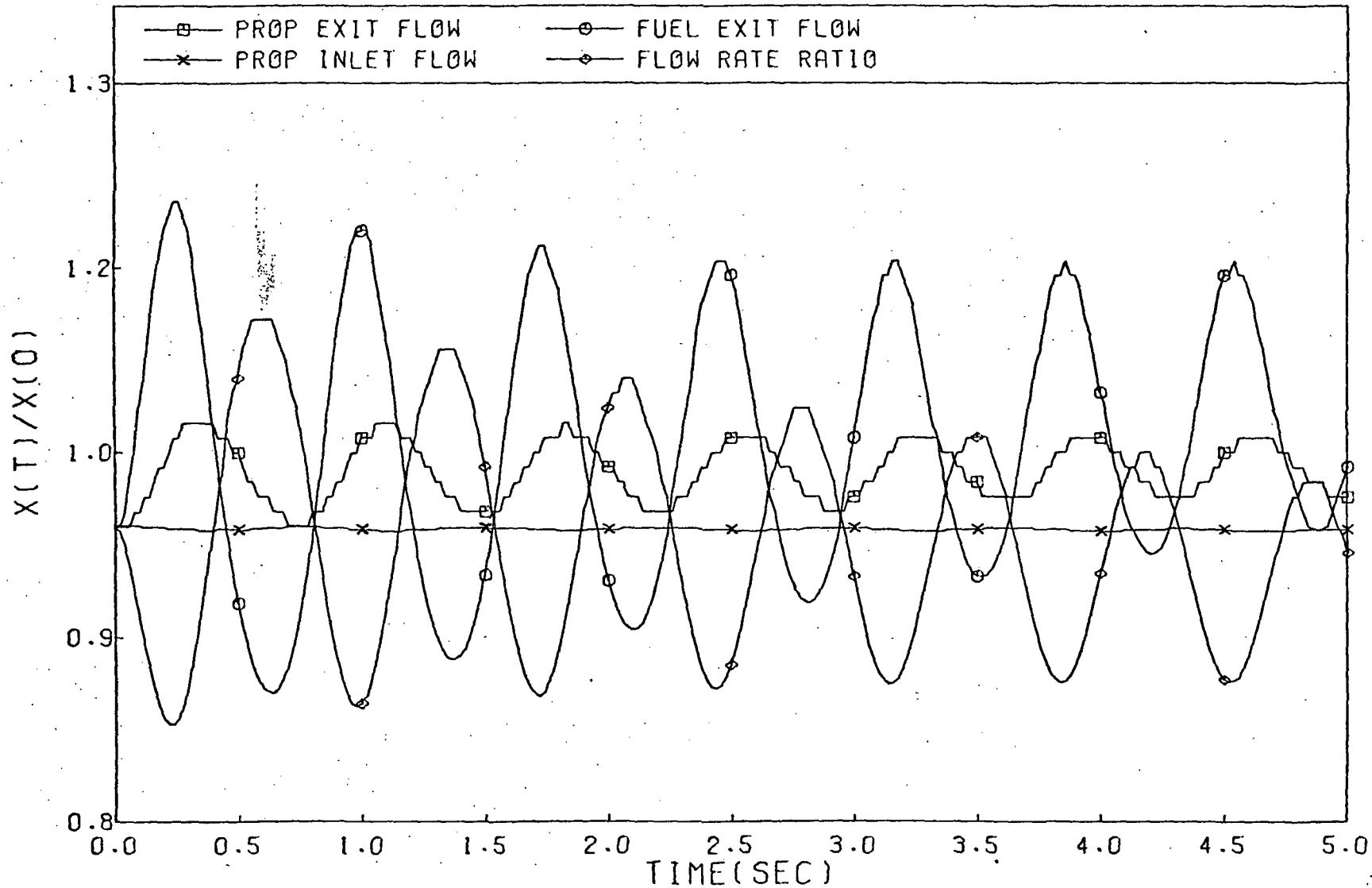

Figure 4-1. Response for Step Insertion of +0.65% Reactivity (cont.)

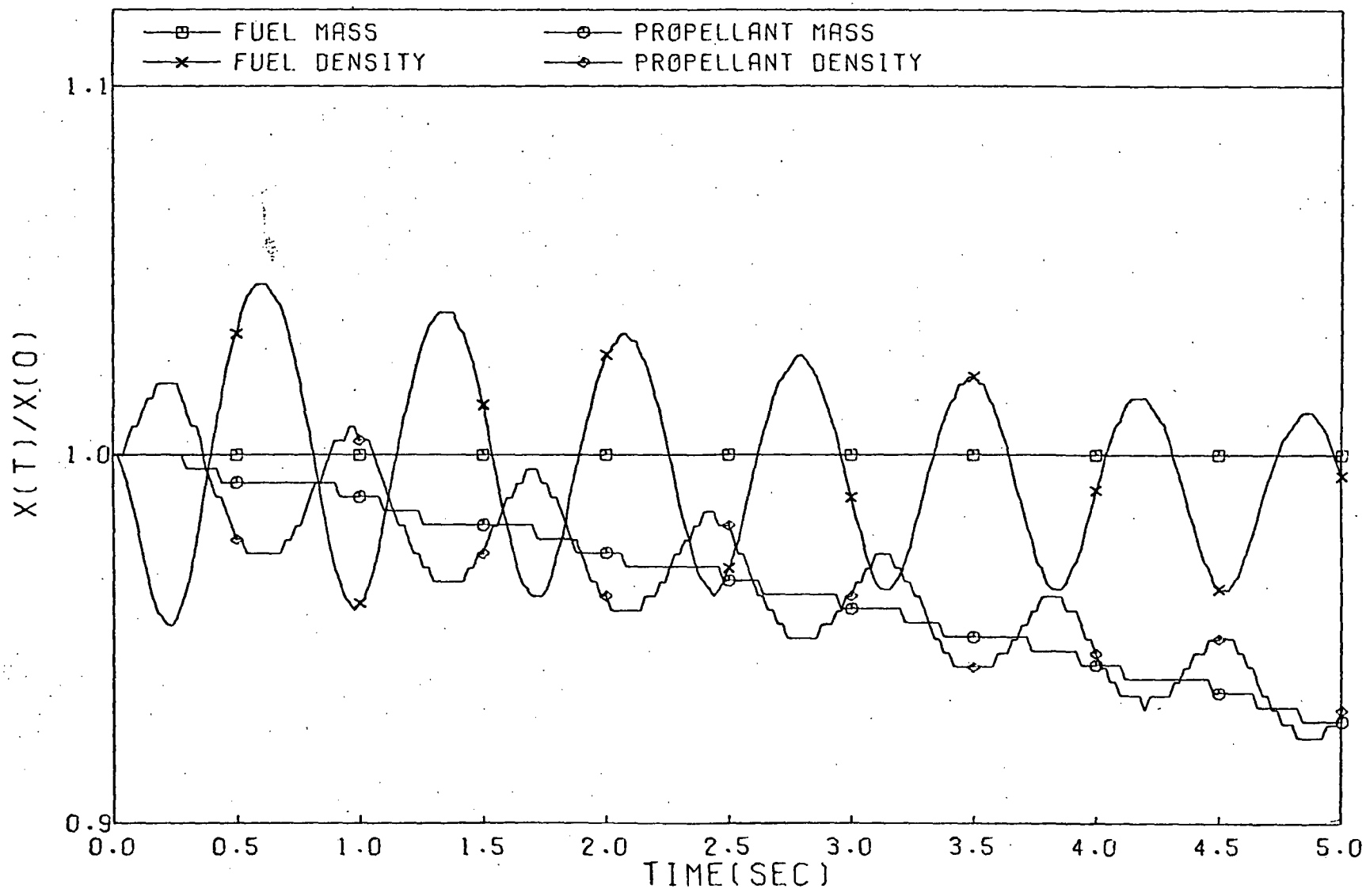

Figure 4-1. Response for Step Insertion of +0.65% Reactivity (cont.)

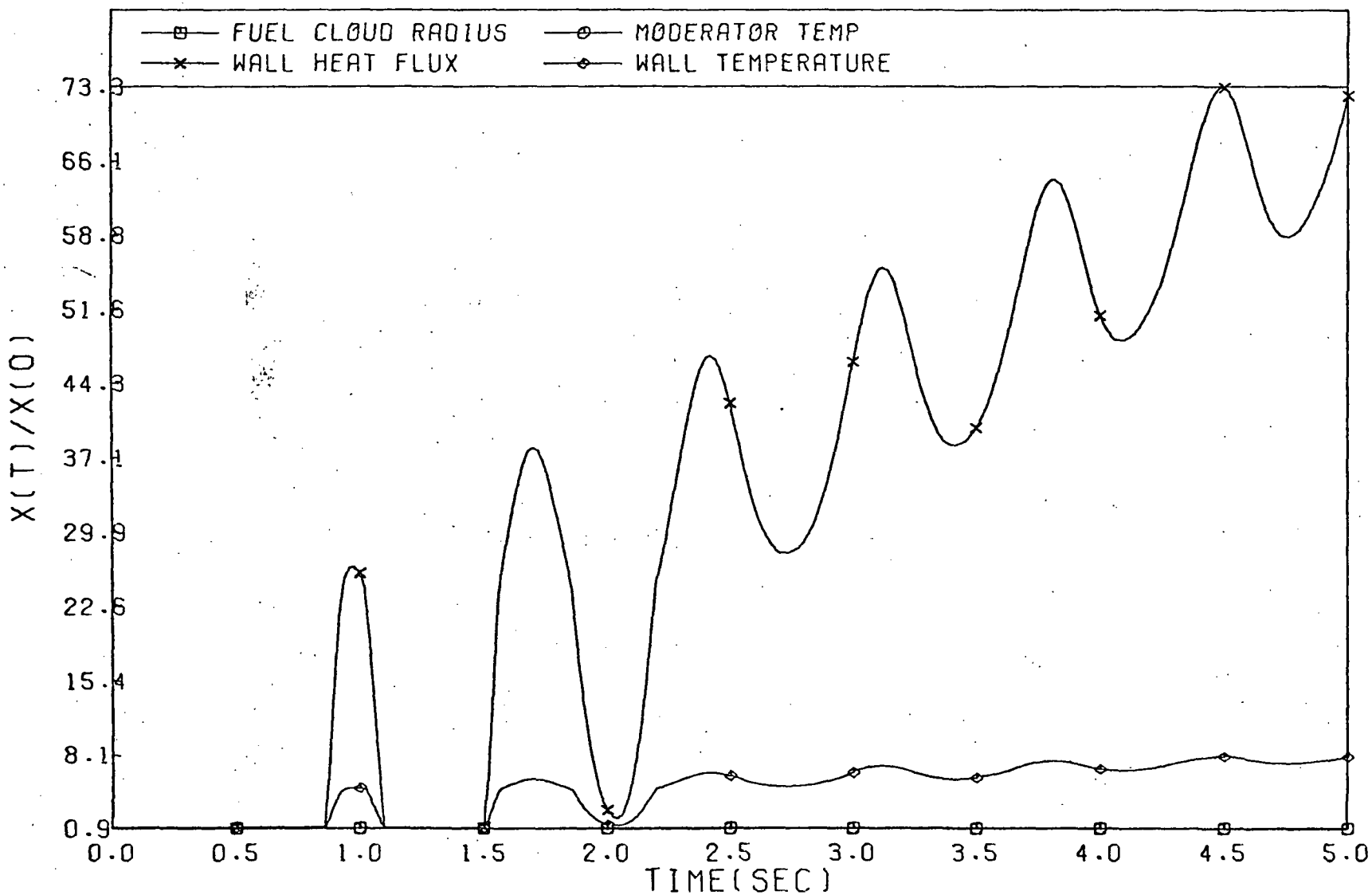

Figure 4-1. Response for Step Insertion of +0.65% Reactivity (cont.)

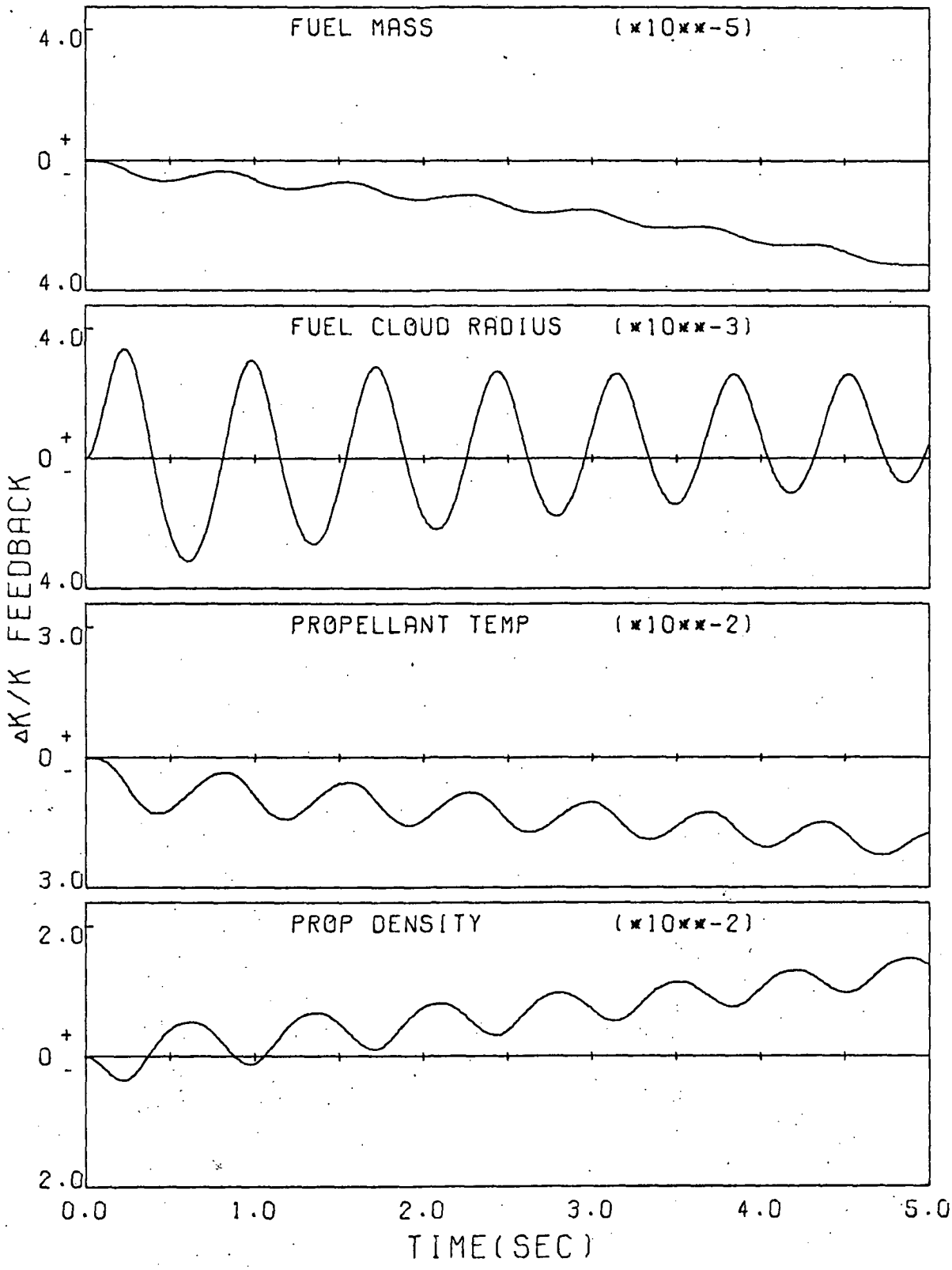

Figure 4-2. Components of Feedback Reactivity Following a Step Insertion of .65% Reactivity

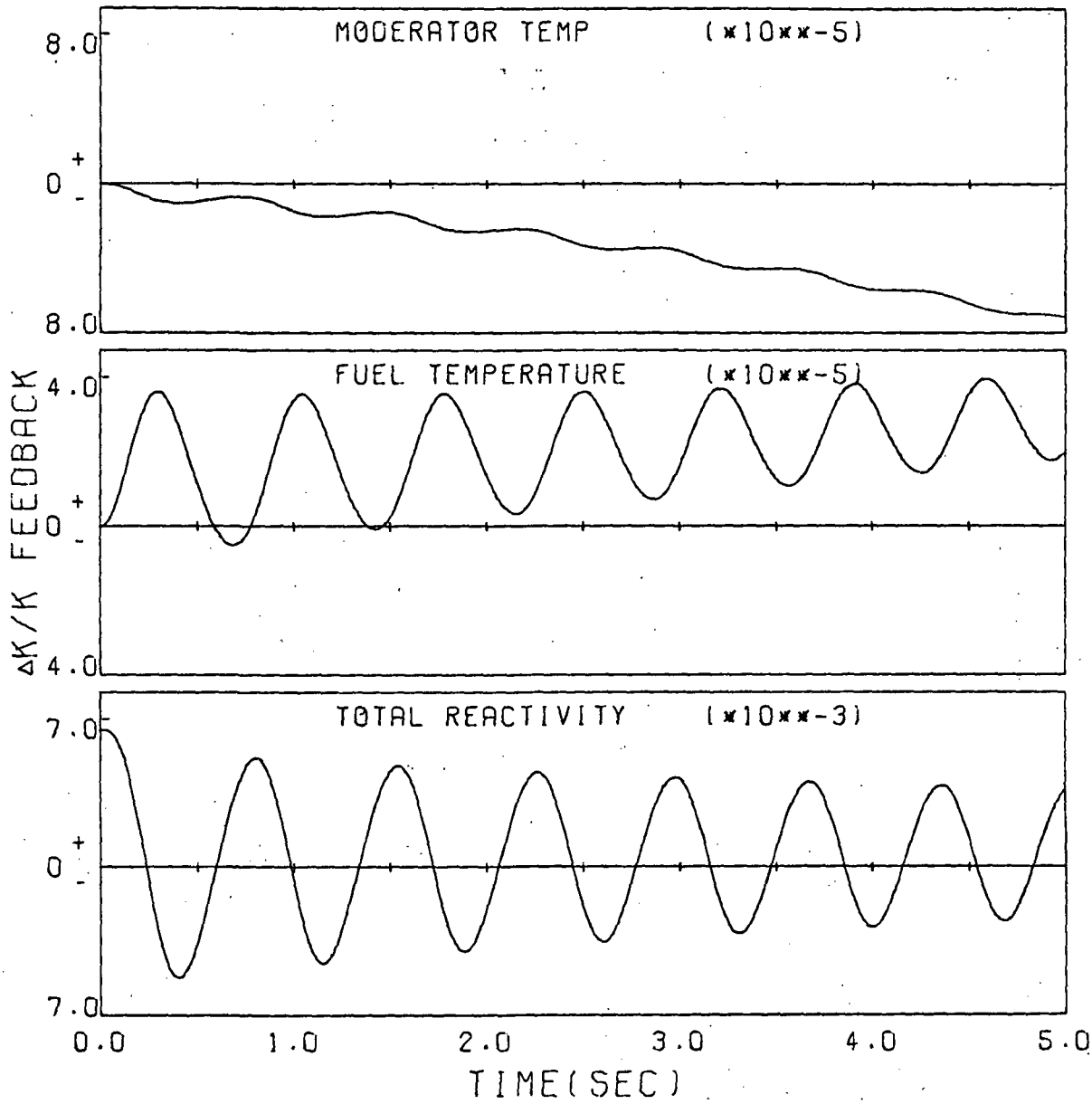

Figure 4-2. (cont.) Components of Feedback Reactivity Following a Step Insertion of .65% Reactivity

the positive reactivity produced by the succeeding power "valley" is still smaller, and so on for each peak and valley combination, with the result that the oscillations are damped. The oscillations of the parameters primarily responsible for reactivity feedback are, however, superimposed upon smaller changes in the average values of the parameters. This is primarily due to the fact that the propellant flow at the cavity exit increases on a time scale much slower than the oscillation period. As a result, after about one second the propellant density has decreased to the point that its reactivity contribution is permanently positive. The negative propellant temperature contribution is insufficient to offset positive feedback from both fuel expansion and propellant density effects, and therefore, the average power increases.

Not surprisingly, the responses obtained with varied fuel mass and moderator temperature coefficients differed negligibly from that indicated in Figure 4-1. This result is consistent with the aforementioned fact that reactivity feedback due to changes in fuel mass and moderator temperature do not contribute appreciably to the overall system response. The reason for the insensitivity to change in these coefficients is that the parameters themselves vary very little after the perturbation, the fuel mass because the fuel injection and ejection rates are very small in comparison to the contained mass and the moderator temperature because of its huge mass.

The model showed perhaps the greatest sensitivity to variations in the propellant temperature coefficient. The reactor response using $\alpha_{T_p} = -.05$ is shown in Figure 4-3. Obviously there is an increasingly rapid rise in power after about 0.8 seconds; cavity pressure reaches 110% of steady state at about .25 seconds, and cavity wall burnout occurs at .375 seconds. The initial power rise is slightly higher than that observed in Figure 4-1 because of the smaller absolute value of α_{T_p}, but, since the propellant temperature feedback

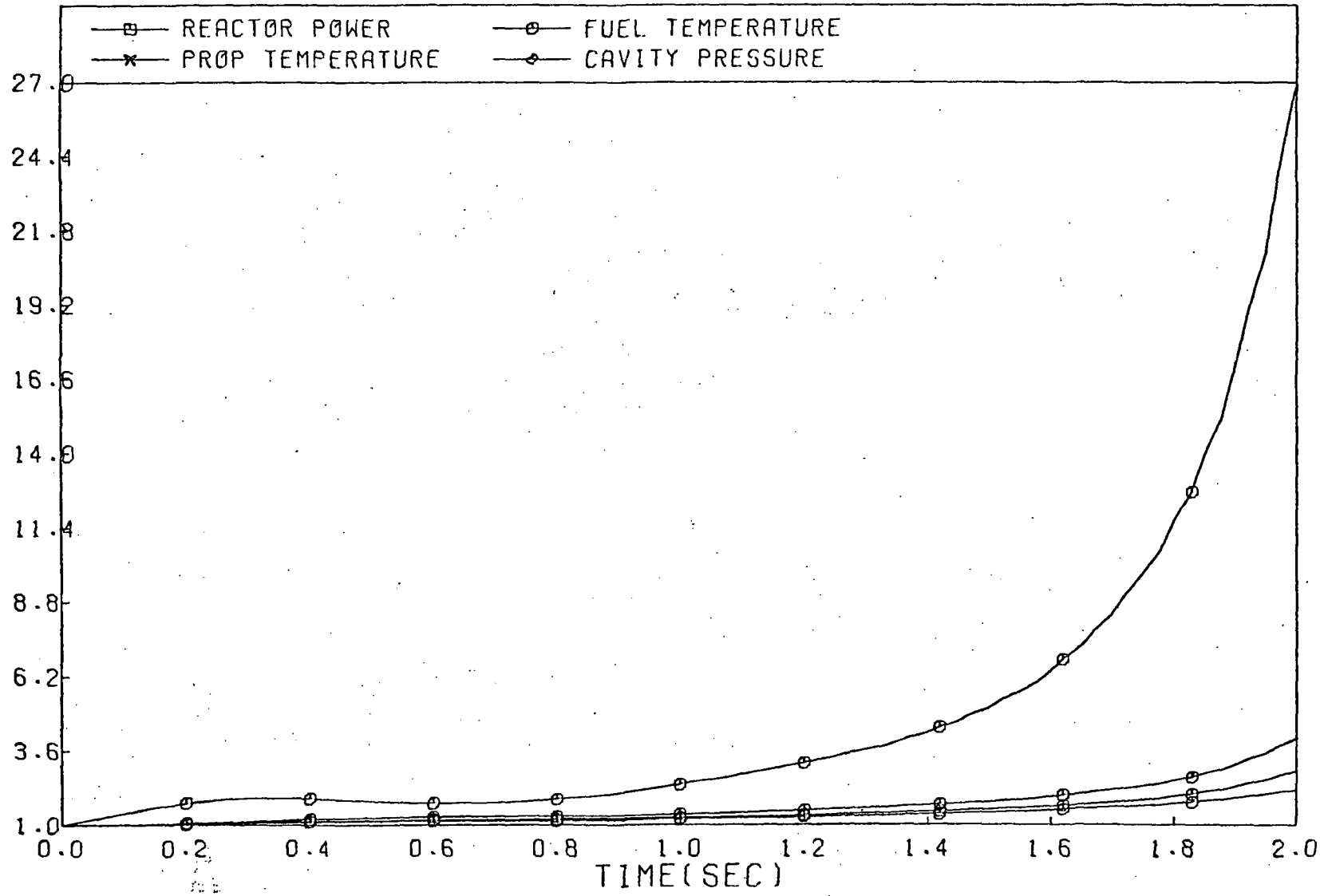

Figure 4-3. Reactor Response with a Propellant Temperature Coefficient of -0.05.

contribution is more significant at later times, the result of Figure 4-3 differs most from reference response at times later than 0.5 second. With the smaller negative propellant temperature coefficient, the increase in positive fuel expansion and propellant density contributions due to power increases is not offset by propellant temperature effects as is the case in Figure 4-2, and the reactor is driven to higher and higher power levels.

Decreasing the value of α_{T_p} to -.5 produced the response depicted in Figure 4-4. The larger propellant temperature feedback coefficient reduces somewhat the size of the initial power peak and also causes the following power valley to occur at a level considerably below that observed when using the reference coefficients. The larger power drop, coupled with the more negative α_{T_p}, produces more positive reactivity which, in turn, drives the power to still higher values. This process continues until the power peaks reach about five times steady state and the power valleys about 10% of the design level. Cavity pressure reaches 10% above design first at about 0.8 seconds; wall burnout first occurs at about 0.73 seconds.

It is apparent that some kind of limiting mechanism takes effect between 1.5 and 2.0 seconds after the perturbation to bracket the power between the levels mentioned above. It is also obvious that the reactor spends more time at the low end of the power oscillations than at the upper end, i. e., the peaks of the oscillations are "sharper" than the valleys. These trends can be better understood in conjunction with the corresponding reactivity plots of Figure 4-5.

As the power drops, the fuel temperature, fuel cloud radius, cavity pressure and propellant density all fall. The propellant temperature behaves more sluggishly than the other parameters, and, as can be seen from Figure 4-1, its response curve lags behind the curves for the other parameters. In this case, the increased rapidity of the first power fall causes the propellant temperature to

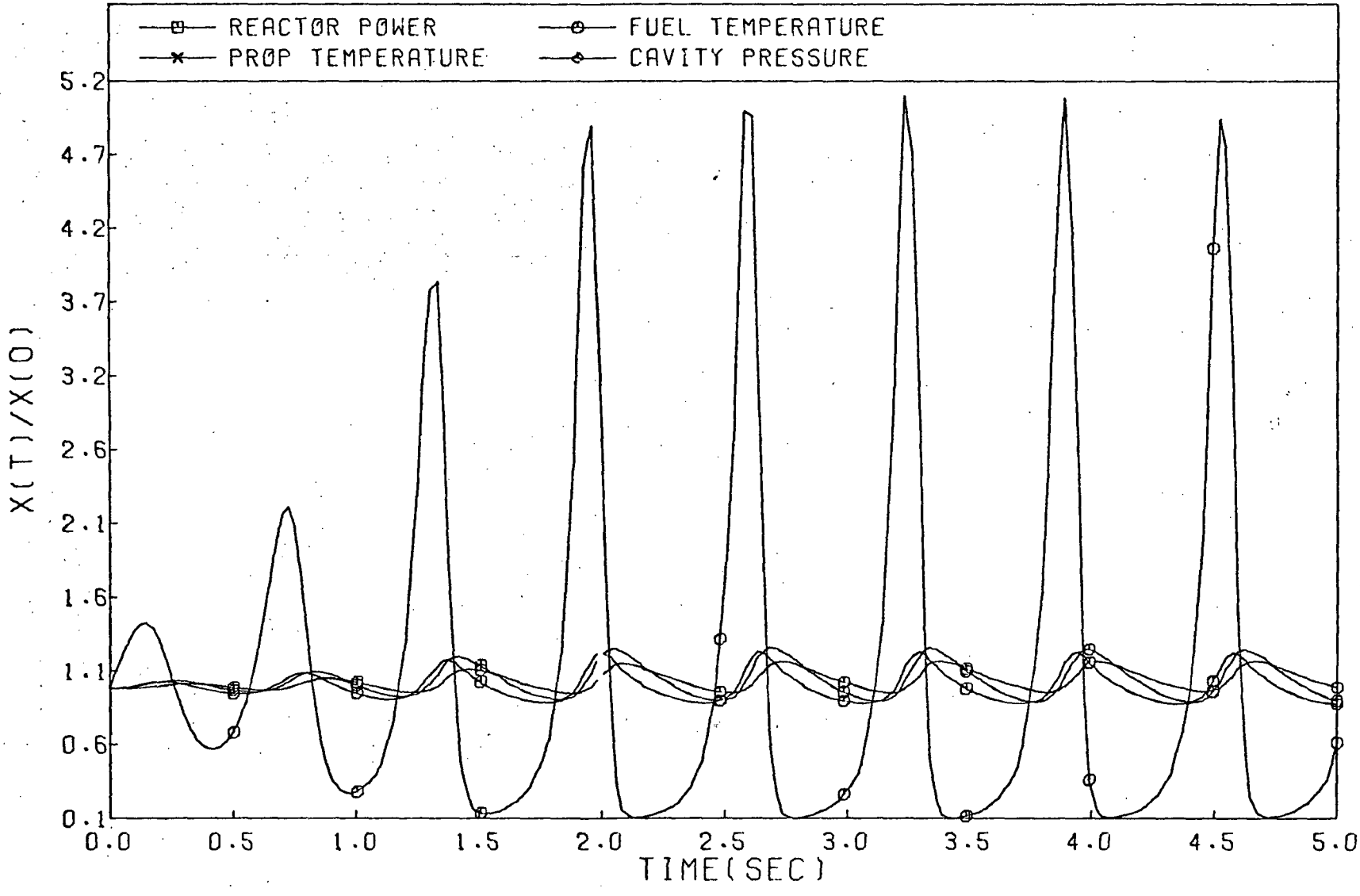

Figure 4-4. Response for a Step Insertion of .65% Reactivity with $\alpha_{T_p} = -.5$

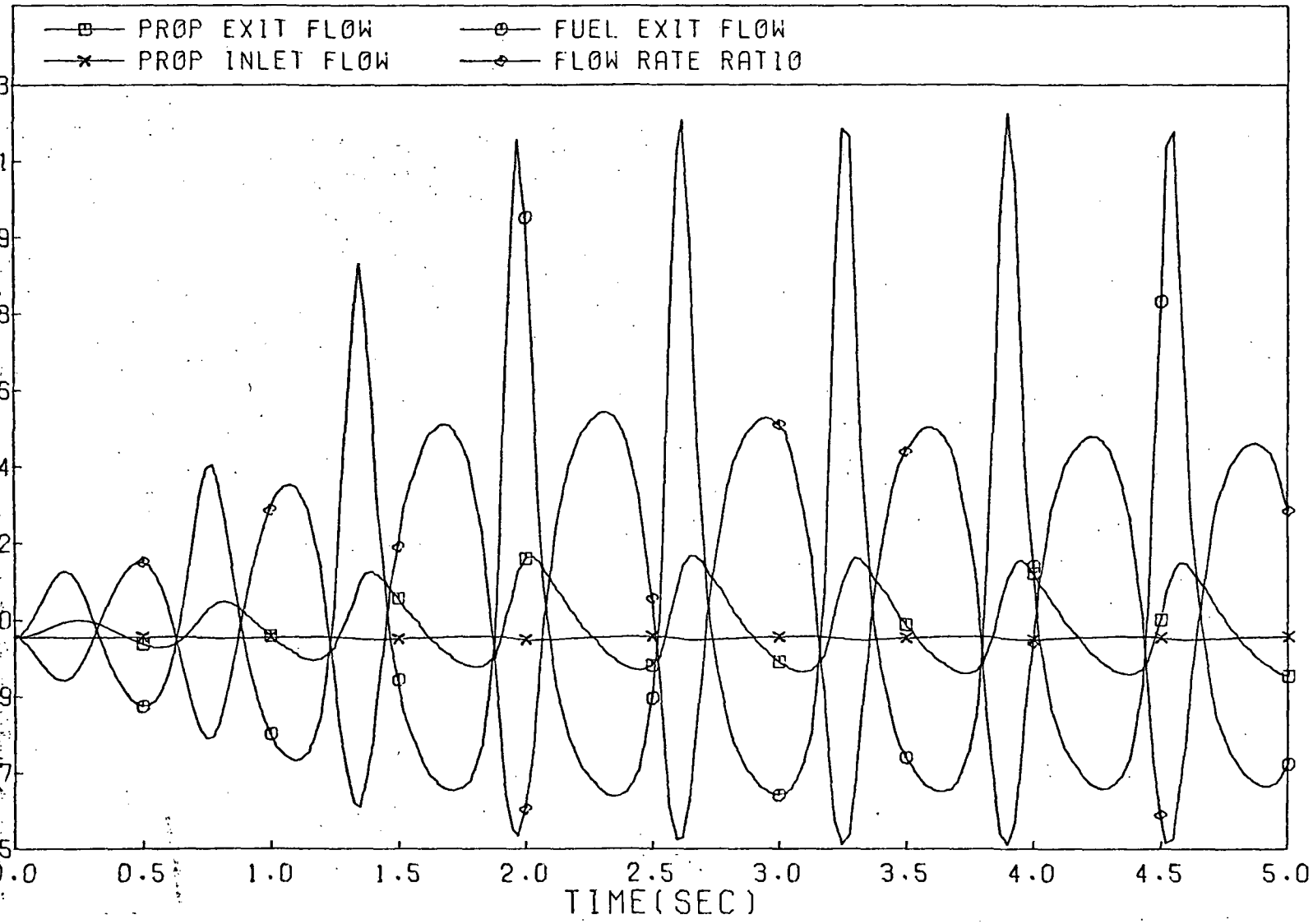

Figure 4-4. Response for a Step Insertion of .65% Reactivity with $\alpha_{T_p} = -.5$

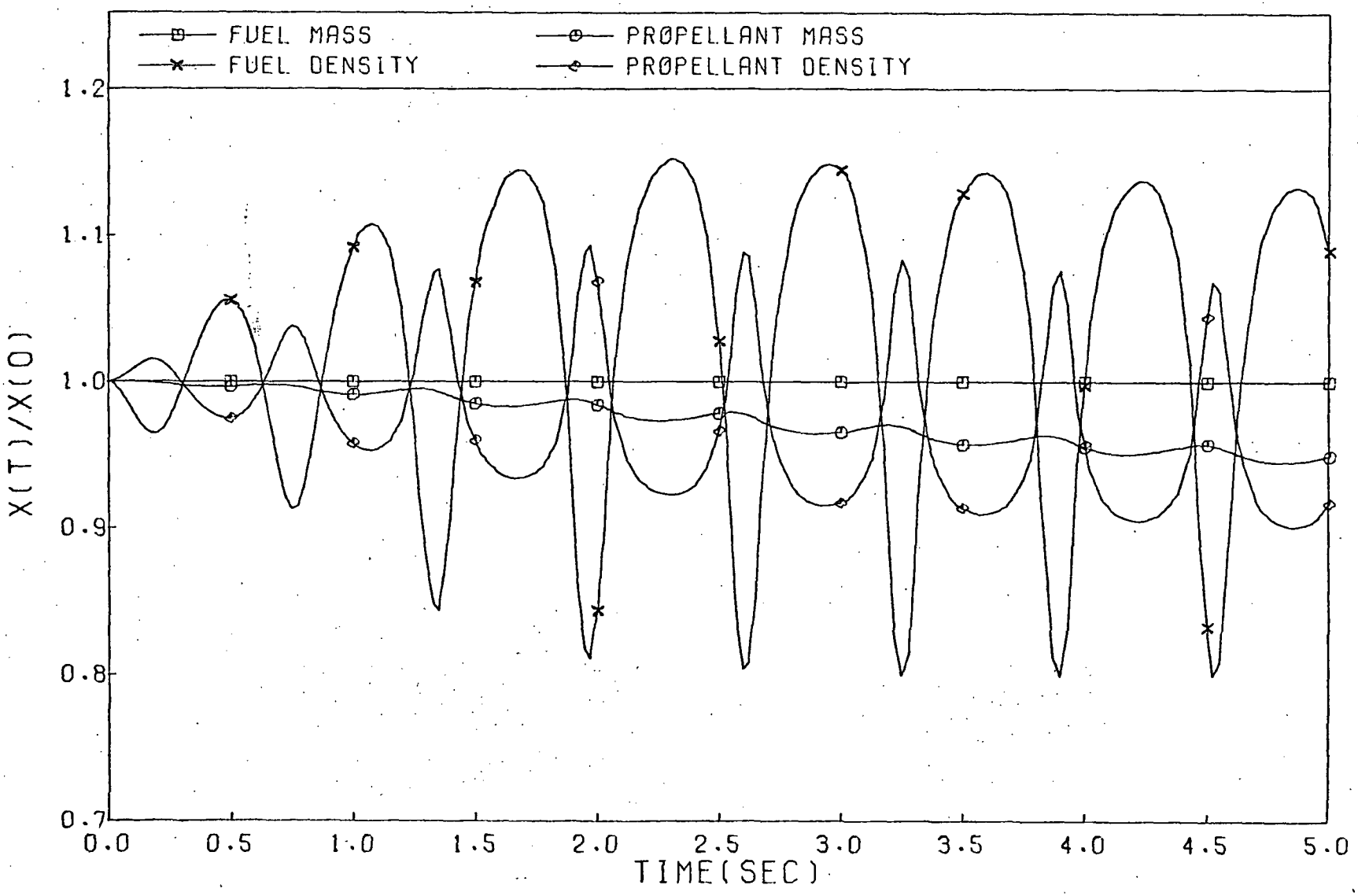

Figure 4-4. Response for a Step Insertion of .65% Reactivity with $\alpha_{T_p} = -.5$

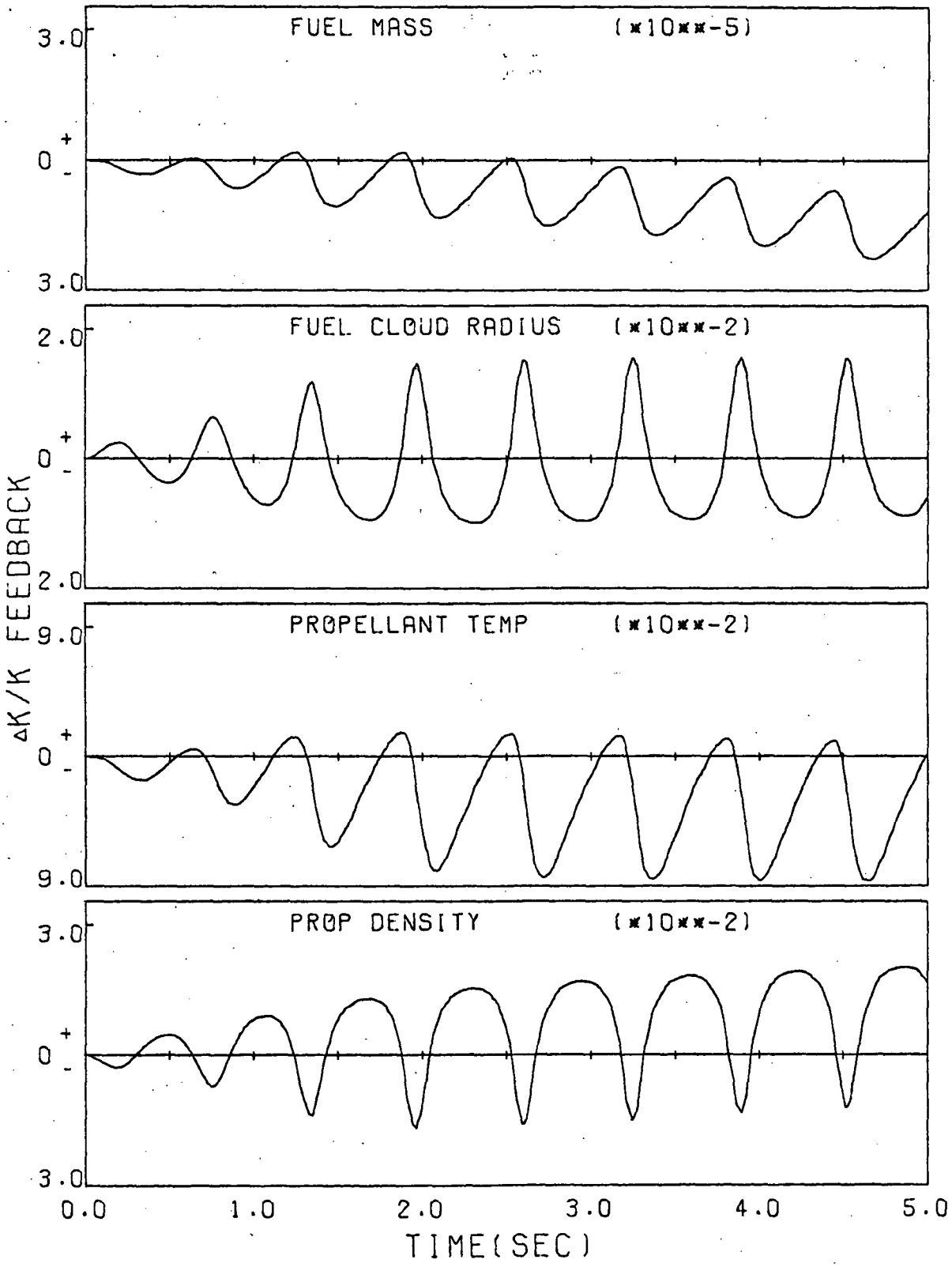

Figure 4-5. Components of Feedback Reactivity for a Step Insertion of .65% Reactivity with $\alpha_{T_p} = -.5$

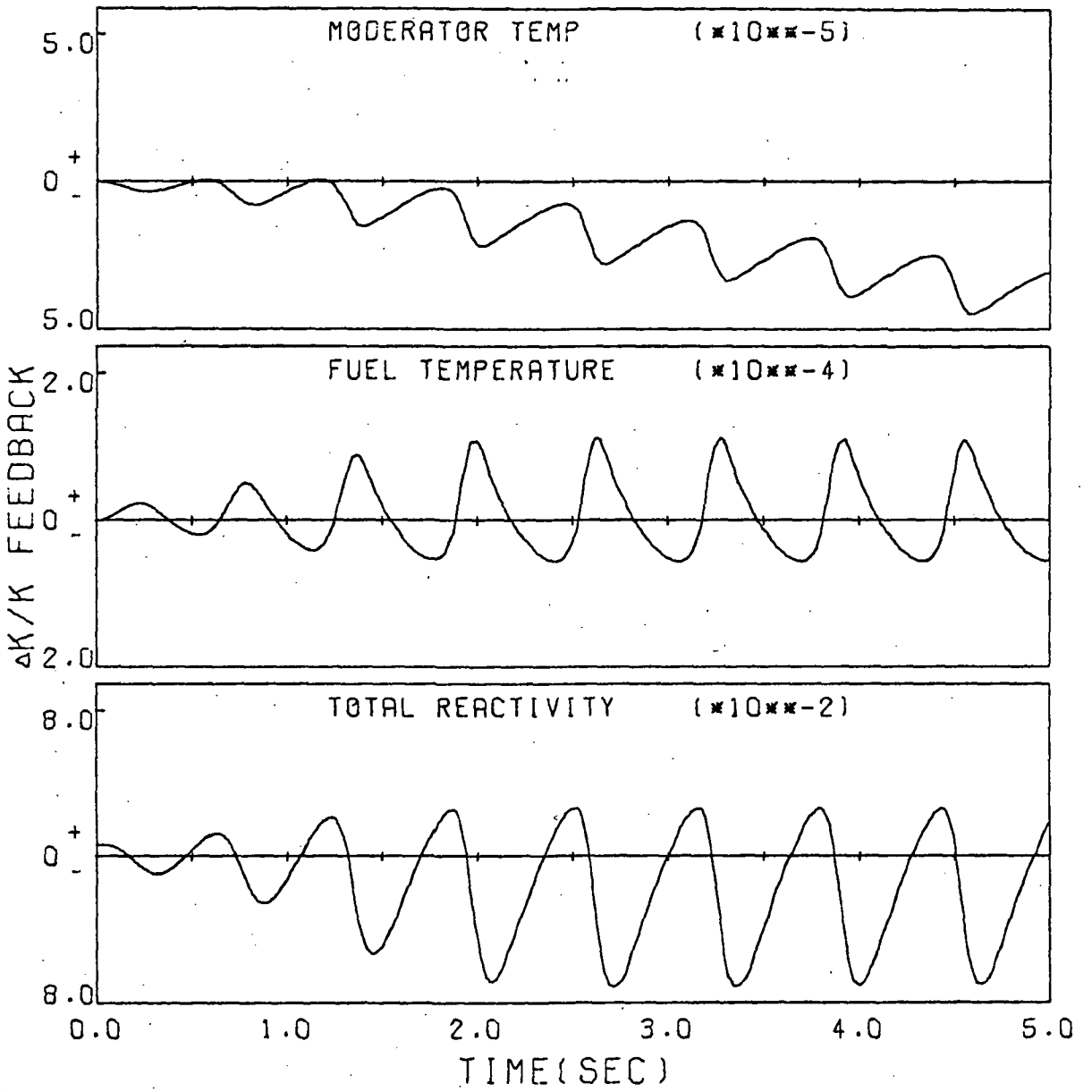

Figure 4-5. Components of Feedback Reactivity for a Step Insertion of .65% Reactivity with $\alpha_{T_p} = -.5$

lag even farther behind the power response. The propellant temperature also drops slower with respect to the cavity pressure; this results in a significant increase in the rate at which the propellant exit flow drops. In this case the propellant ejection rate actually falls below its design value, which leads to an increase in contained propellant mass. Neither of these phenomena occur when the reference coefficients are used. The increase in propellant mass causes a retardation in the rate of propellant temperature and density decreases, which, in turn, cause a corresponding reduction in the rate of positive reactivity insertion. As the propellant temperature does begin to drop, however, the above mentioned retardations become less and less significant and positive reactivity is inserted more and more rapidly. Due to the net decrease in contained propellant mass, the resulting positive insertion is larger than the original and the power rises to a higher value. The propellant temperature tends to follow the power rises more closely than the power drops because the contained propellant mass is at or near its lowest values when the temperature is rising.

The mechanisms described above which cause the behavior depicted in Figure 4-4 tend to be self enhancing so that the asymmetric behavior becomes more pronounced with each oscillation up to about two seconds after the perturbation. At this time the negative reactivity inserted by the power peaks produces valleys which, in turn, produce peaks identical to the one previous. Thus the reactor has acheived a state of repeated asymmetric oscillations which characterize the behavior of the reactor for succeeding times.

From the above discussion, it is clear that any increase in the rate at which the power falls from the first peak will tend to produce a similar response. It can be seen from Figures 4-1 and 4-2, which depict the response using the reference coefficients, that a decrease in fuel cloud radius contributes to the drop in power while a drop

in propellant density simultaneously opposes it. Hence, one would suspect that increasing α_{r_f} or decreasing the absolute value of α_{ρ_p} might produce results similar to those of Figure 4-4. As can be seen from Figures 4-6 and 4-7, which are, respectively, the responses to a step insertion of .65% reactivity using the values $\alpha_{r_f} = .3$ and $\alpha_{\rho_p} = -.1$, the same type of asymmetrical oscillatory response is, in fact, obtained. For the case $\alpha_{\rho_p} = -.1$, the period of the oscillation is slightly longer than the response of Figure 4-4; increasing α_{r_f} to a value of .3 causes a delay in reaching the "balanced" oscillation stage. The peak power obtained in both of these responses is about 3.9 times steady state whereas for $\alpha_{T_p} = -.5$ the peak power reached 5.2 times the design value.

Not surprisingly, the response obtained with $\alpha_{\rho_p} = .2$ (instead of .19) was negligibly different from that shown in Figure 4-1.

The response using $\alpha_{r_f} = .15$ is shown in Figure 4-8. The reactor power oscillates at about the same frequency as was characteristic of the response using the reference coefficients. However, the oscillations are damped somewhat faster than in the reference case; the reason for the additional damping can be ascertained through examination of Figures 4-1 and 4-2. It will be noted that the fuel cloud radius reactivity feedback component tends to follow the behavior of the reactor power, that is, when the power is rising the feedback reactivity from this component is rising and vice versa. Thus, feedback from this component tends to drive the reactor to higher power levels when the power is rising and to lower power levels when the power is falling. Reducing the size of the fuel expansion coefficient reduces the feedback from changes in the fuel cloud radius and, therefore, reduces the reactor's tendency to oscillate.

Increased damping in the behavior of the reactor power is even more evident when the response obtained by substituting the reference value of the fuel temperature coefficient with $\alpha_{T_f} = -.5$. (see Figure 4-9). As with the fuel expansion coefficient, the fuel temperature feedback tends to follow the reactor power; however, when using the reference value, the

overall effect of the fuel temperature feedback on the reactor's behavior is not great. When $\alpha_{T_f} = -.5$ is used, the situation is exactly the opposite. The dramatically increased size of α_{T_f} makes fuel temperature feedback large enough to compete with fuel expansion and propellant density and temperature as a determiner of reactor behavior. Additionally the reversal in sign causes fuel temperature feedback to oppose each power oscillation rather than to enhance it. Thus, not only is the initial peak curtailed significantly, but the reactor response is so sharply damped that essentially all oscillations are gone after about 1.5 seconds.

Changing α_{T_f} from .001 to .002 did not alter the reactor's response.

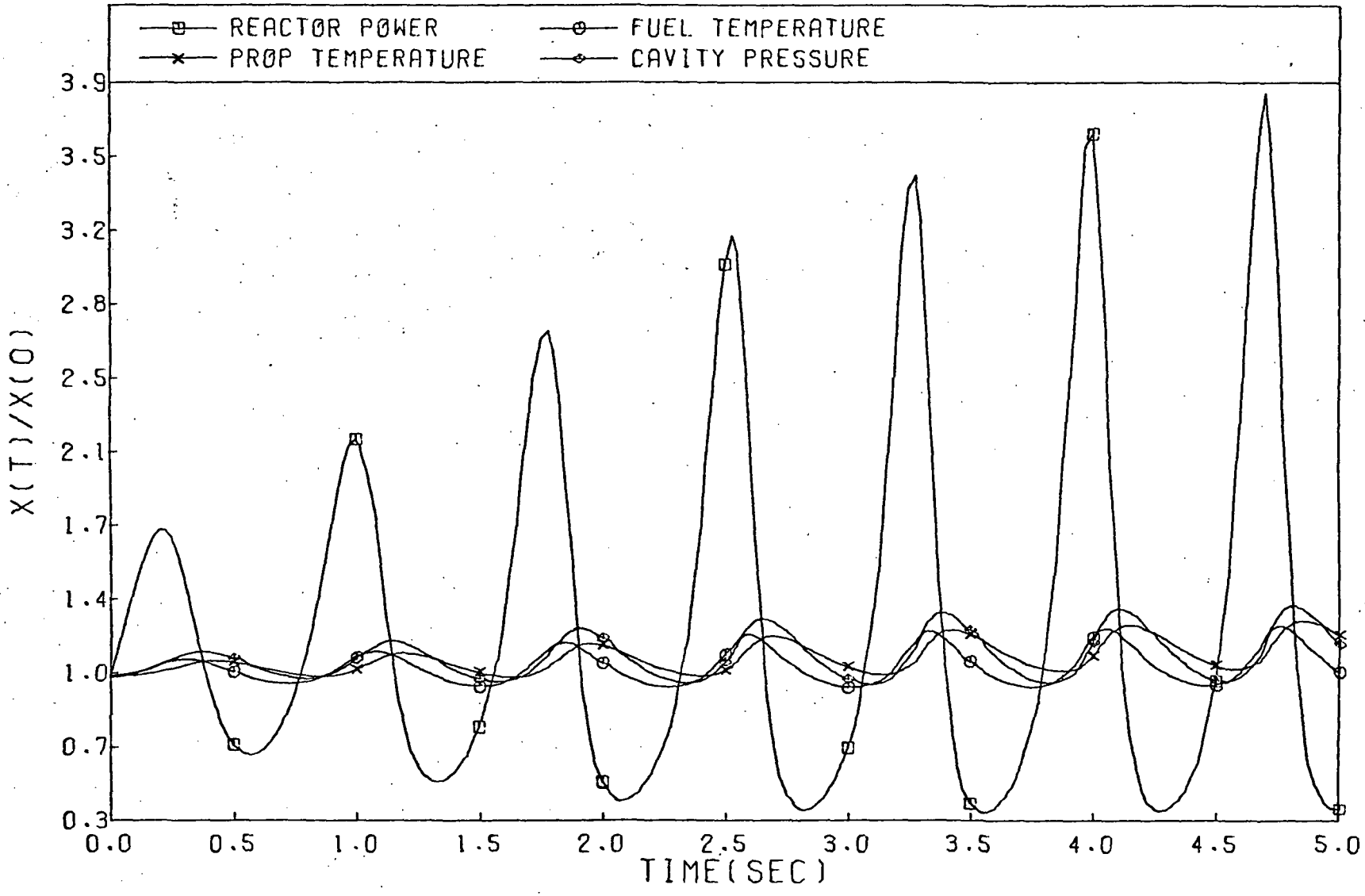

Figure 4-6. Response for a Step Insertion of .65% Reactivity with α_{r_f} = .3

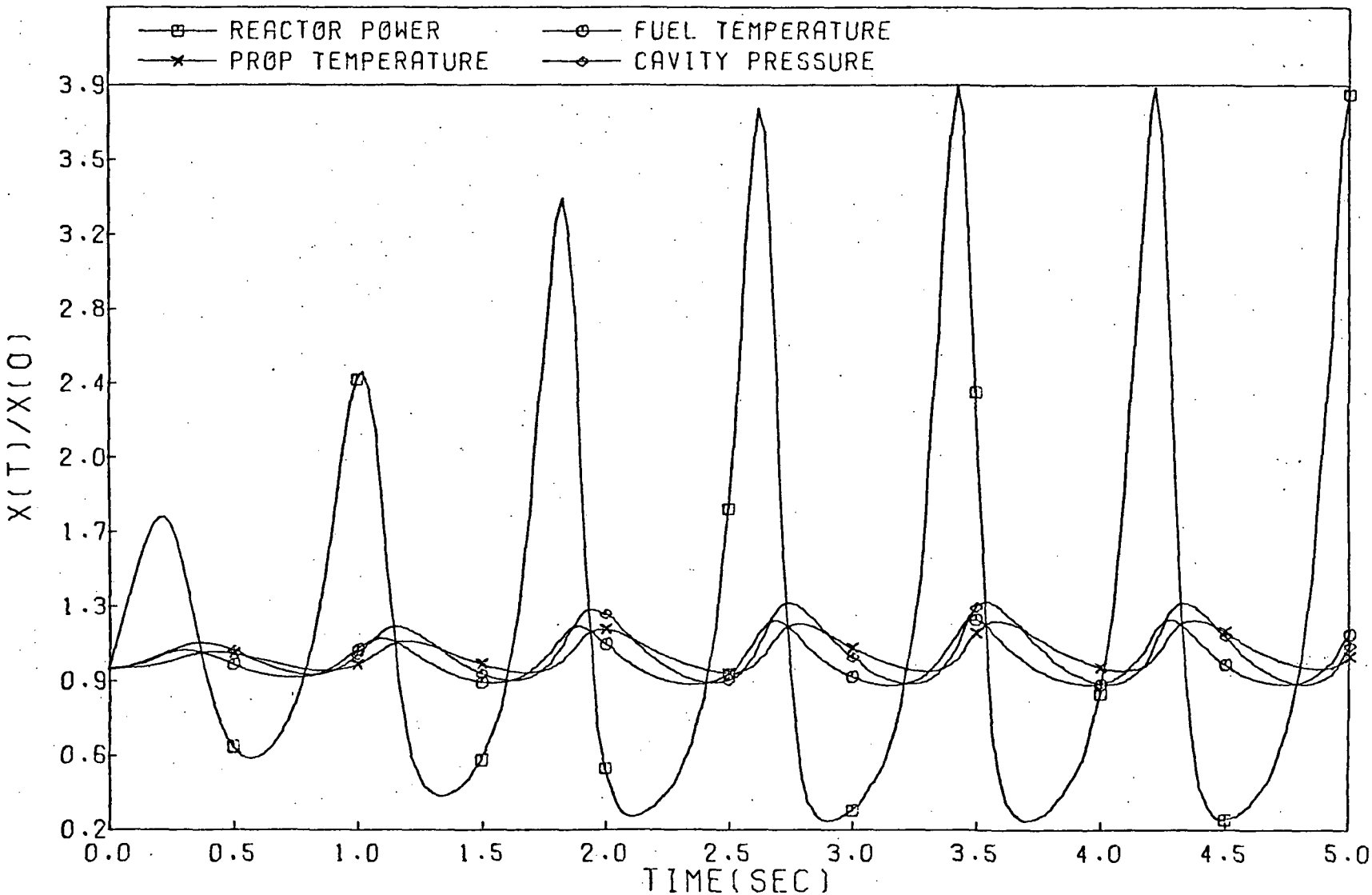

Figure 4-7. Response for a Step Insertion of .65% Reactivity with $\alpha_{\rho_p} = -.1$

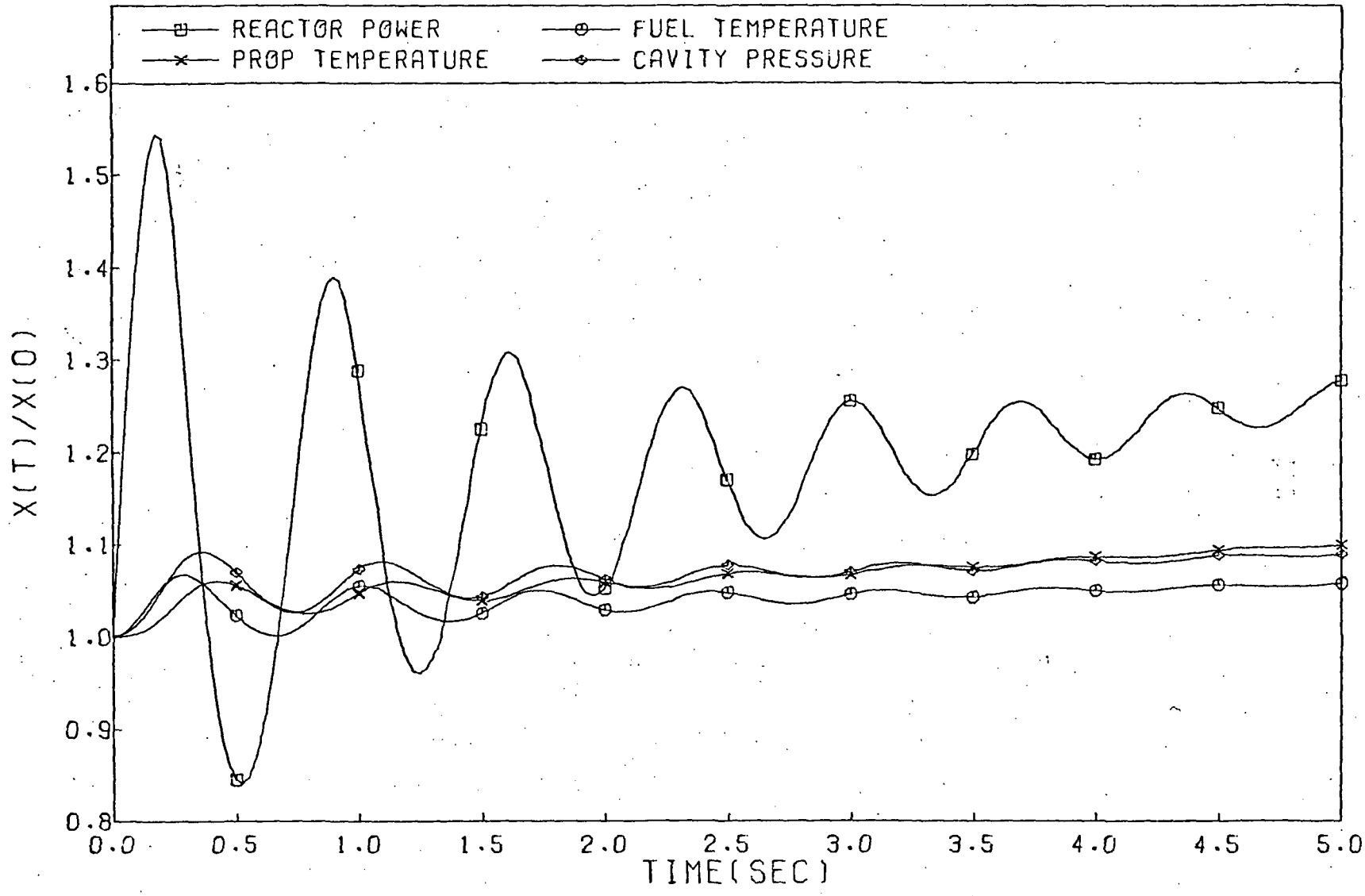

Figure 4-8. Response for a Step Insertion of .65% Reactivity with α_{r_f} = .15

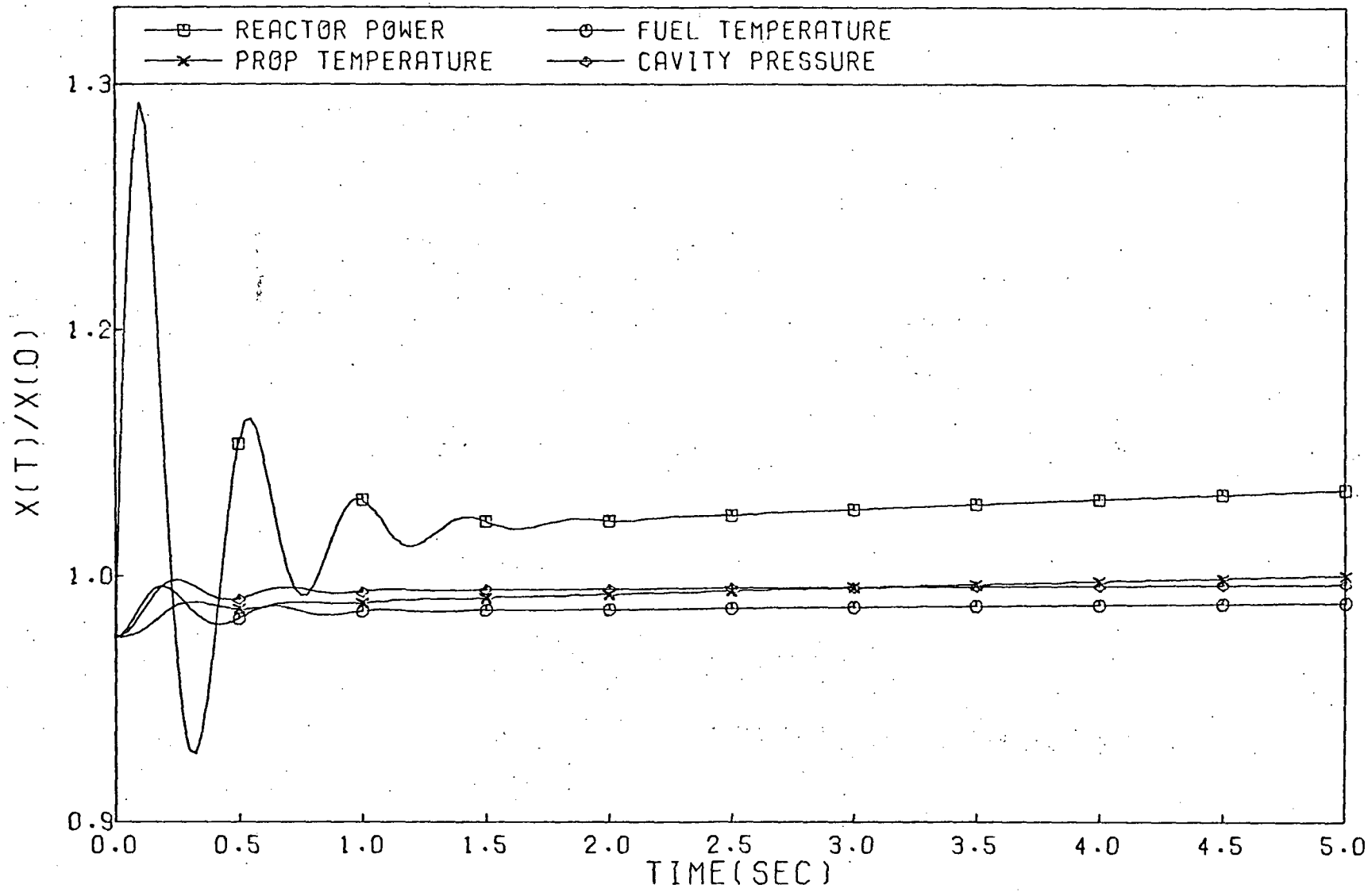

Figure 4-9. Response for a Step Insertion of .65% Reactivity with $\alpha_{T_f} = -.5$

Section 5

THE RESPONSE OF THE UNCONTROLLED REACTOR

Using the reference reactivity coefficients, CØDYN II was used to predict the response of the reactor to several perturbations. Responses for reactivity insertions of ± .65%, ± .2%, ± .1%, and ± .05% and changes of ± 5, 10, and 20 per cent in the fuel and propellant injection rates were predicted. The following is a summary of the results obtained for these twenty perturbations.

Ractivity Insertions

The response for a reactivity insertion of .65% was described in detail in Section 4.

A negative step insertion of .65% reactivity produces the response depicted in Figure 5-1; the corresponding reactivity plots appear in Figure 5-2. The response is, again, a damped oscillation superimposed, in this case, on a drop in average power. The oscillations are damped somewhat faster in the negative reactivity insertion case, however. As indicated in Figure 5-2, the reactivity effects are basically opposite to those encountered in Figure 4-2. The apparent reason for the increased damping is that the decrease in fuel cloud radius and propellant density caused by the negative insertion are not as great as the increases caused by the positive insertion. Thus, the reactivity feedback for a given power excursion in the negative direction is less than for a corresponding positive deviation, and oscillations for the cases with an initial power decrease are characteristically more sharply damped. Responses for smaller negative reactivity insertions were qualitatively the same as that shown in Figure 5-1; in no case did the wall heat flux rise above the burnout value.

As can be seen from the response to a positive step insertion of .05% reactivity (Figure 5-3), the response to small reactivity insertions is qualitatively the same as that discussed above. The

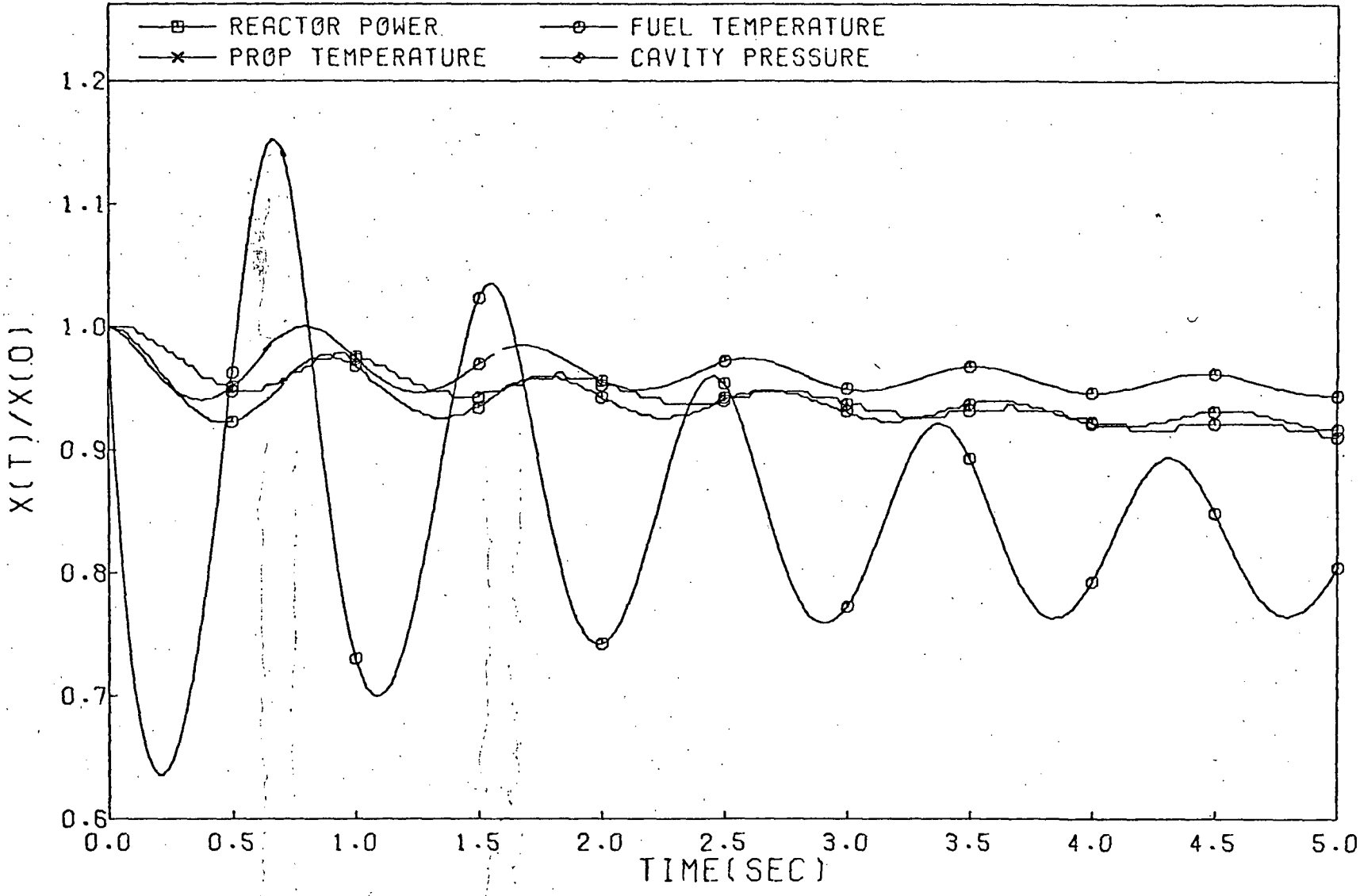

Figure 5-1. Response for a Negative Insertion of .65% Reactivity

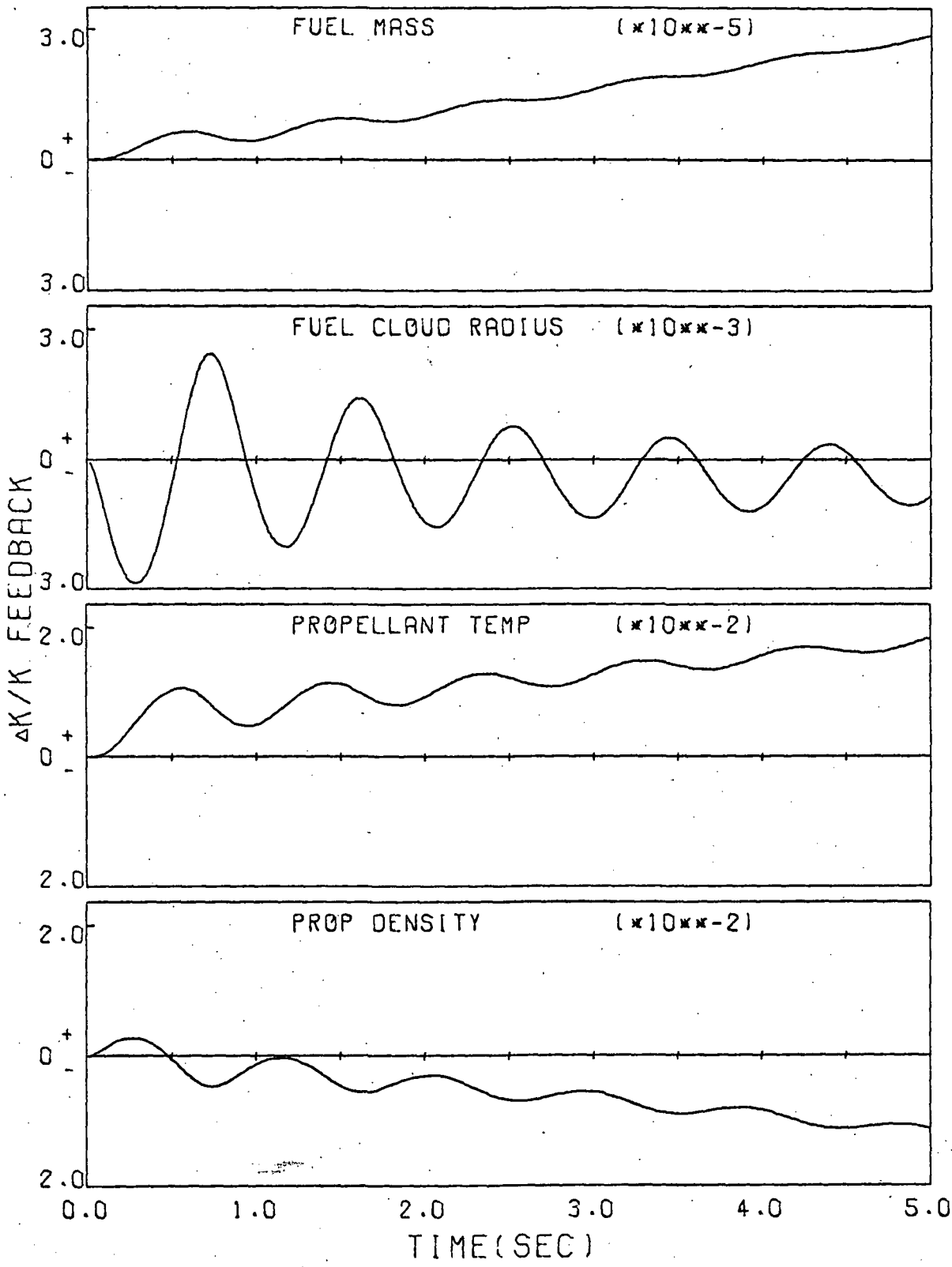

Figure 5-2. Components of Feedback Reactivity Following a Negative Step Insertion of .65% Reactivity

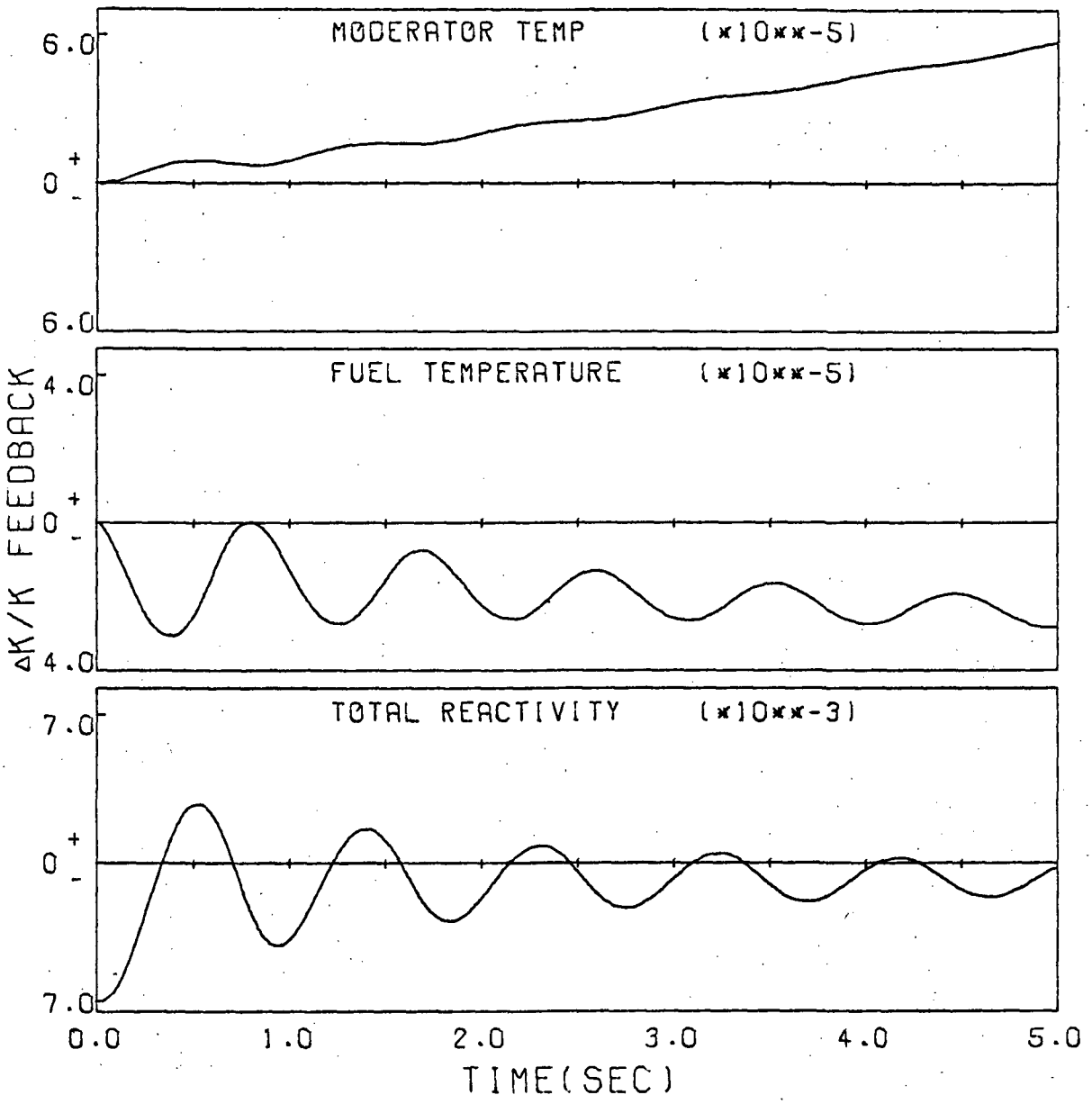

Figure 5-2. Components of Feedback Reactivity Following a Negative Step Insertion of .65% Reactivity

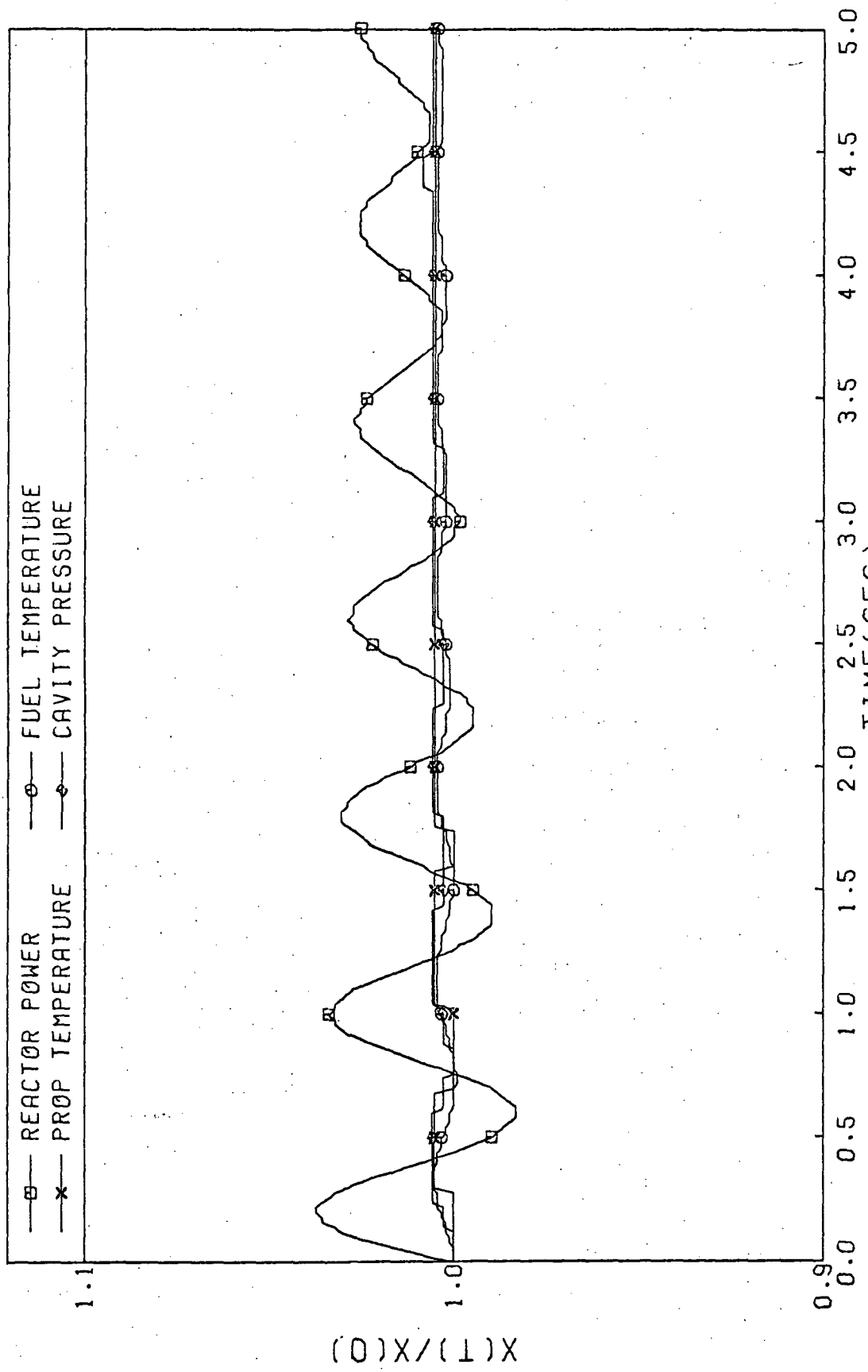

Figure 5-3. Response for a Positive Insertion of .05% Reactivity

initial power peaks were at 3.7%, 7.5% and 15.6% above design for reactivity insertions of .05%, .1%, and .2% respectively; all first peaks occured at about 200 milliseconds. The cavity wall heat flux did not exceed burnout values for any of the smaller insertions, nor did the cavity pressure rise above .73%, 1.5% and 3.14% above steady state for the three smaller reactivity perturbations.

Variations in Injections Rates

The system response to a 20% decrease in propellant injection rate is depicted in Figure 5-4. Like the power behavior after reactivity insertions, the response is oscillatory with a rise in average power. In this case, however, the rise in average power is considerably faster, and the oscillations deviate from the average value somewhat less. Although the initial power peak is only 20% above steady state, the rapid rise in average power causes increases of 200% by 3.5 seconds and 300% by five seconds after the injection rate change. Cavity pressure has increased by ten per cent over the design value by 2.3 seconds, and wall burnout conditions are reached nearly instantaneously. The rapid rise in wall heat flux is due directly to the decrease in propellant injection rate rather than an increase in heat flux from the fuel cloud. As indicated in Figure 5-5, which is the response to a step decrease of 5% in propellant injection rate, the power response is qualitatively similar to that of Figure 5-4. The rise in power is considerably slower in this case, but, again, burnout wall heat flux values are attained nearly instantaneously.

The reactivity effects producing the responses of Figures 5-4 and 5-5 can be understood by examining the feedback plots of Figure 5-6. Decreasing the propellant injection rate causes a drop in propellant density and an expansion of the fuel cloud, both of which are positive reactivity effects. As the power increases, the fuel and propellant temperatures rise. The fairly large negative component produced by the increase in propellant temperature is not adequate to counteract the positive effects. Again, fuel temperature, moderator temperature, and fuel mass effects are not great enough to contribute

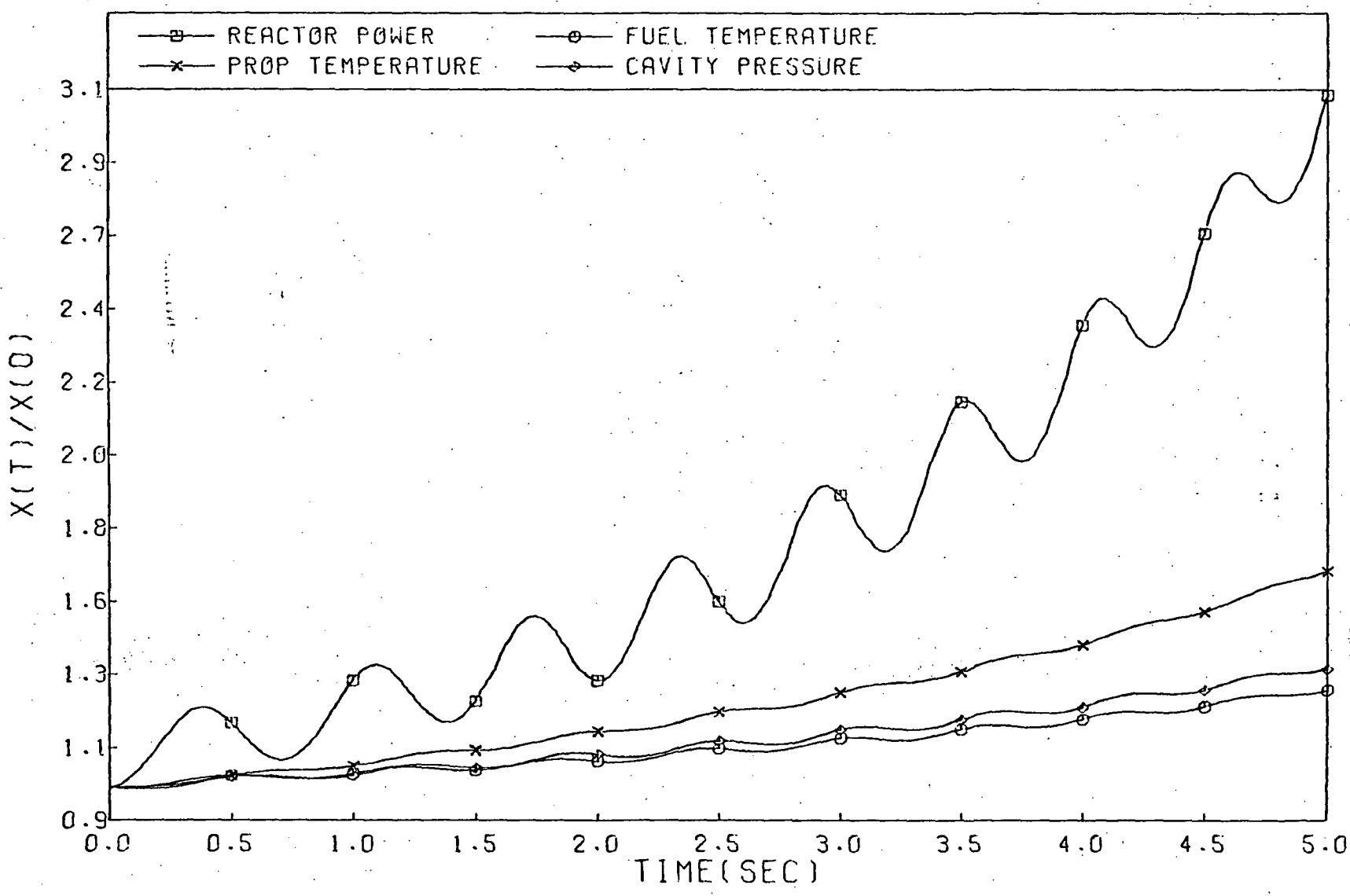

Figure 5-4. Response for a 20% Decrease in Propellant Injection Rate

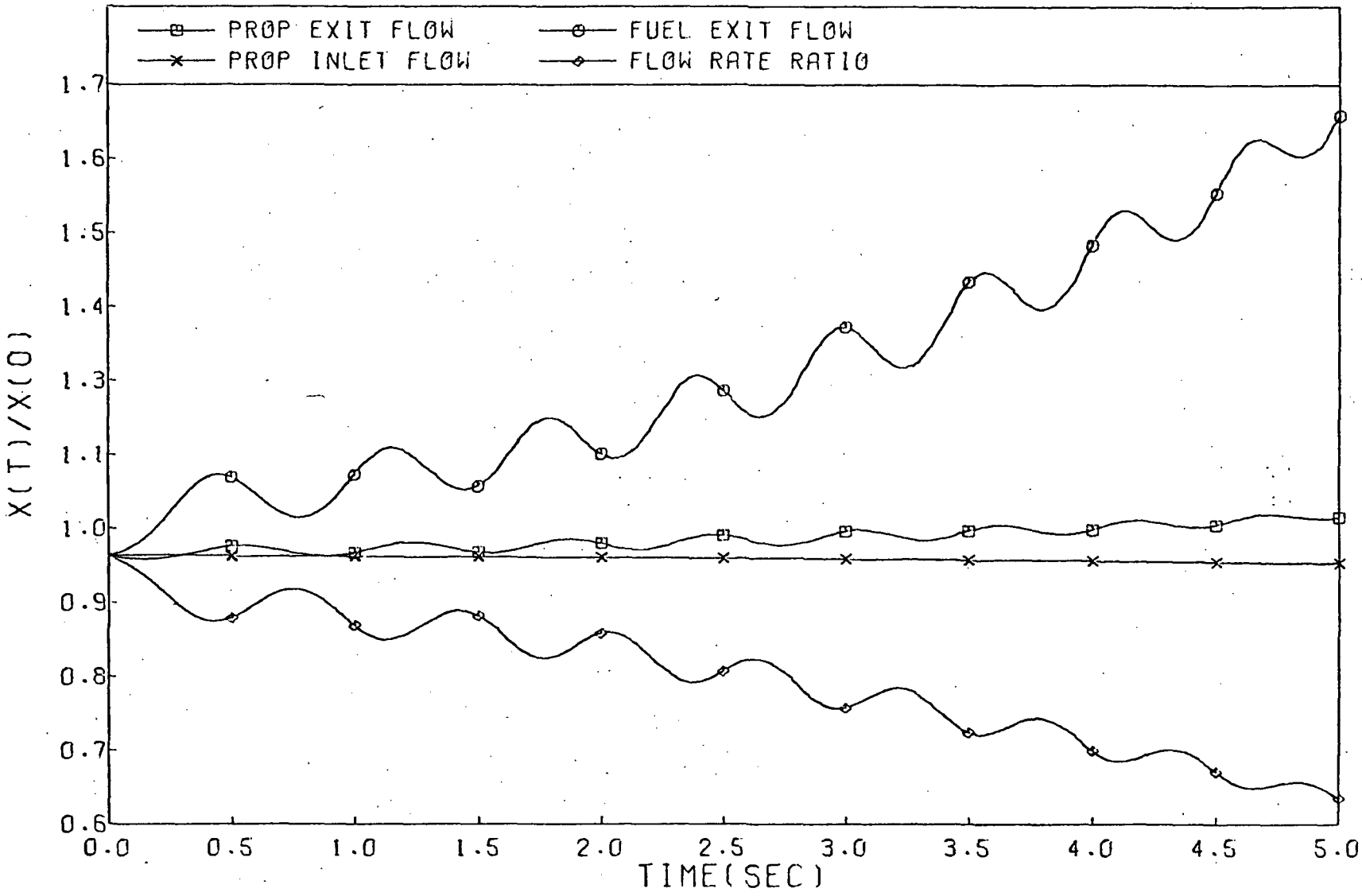

Figure 5-4. Response for a 20% Decrease in Propellant Injection Rate

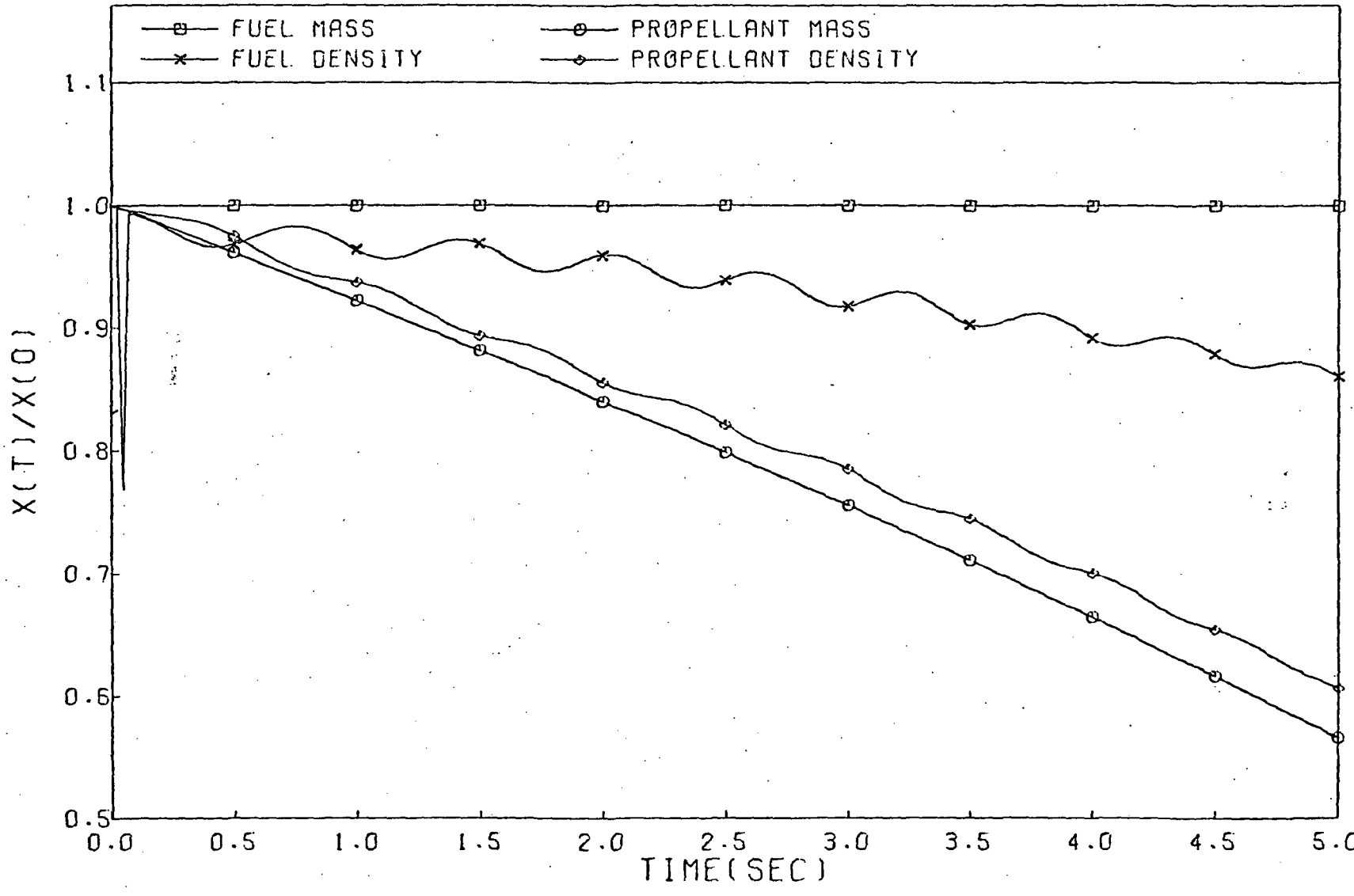

Figure 5-4. Response for a 20% Decrease in Propellant Injection Rate

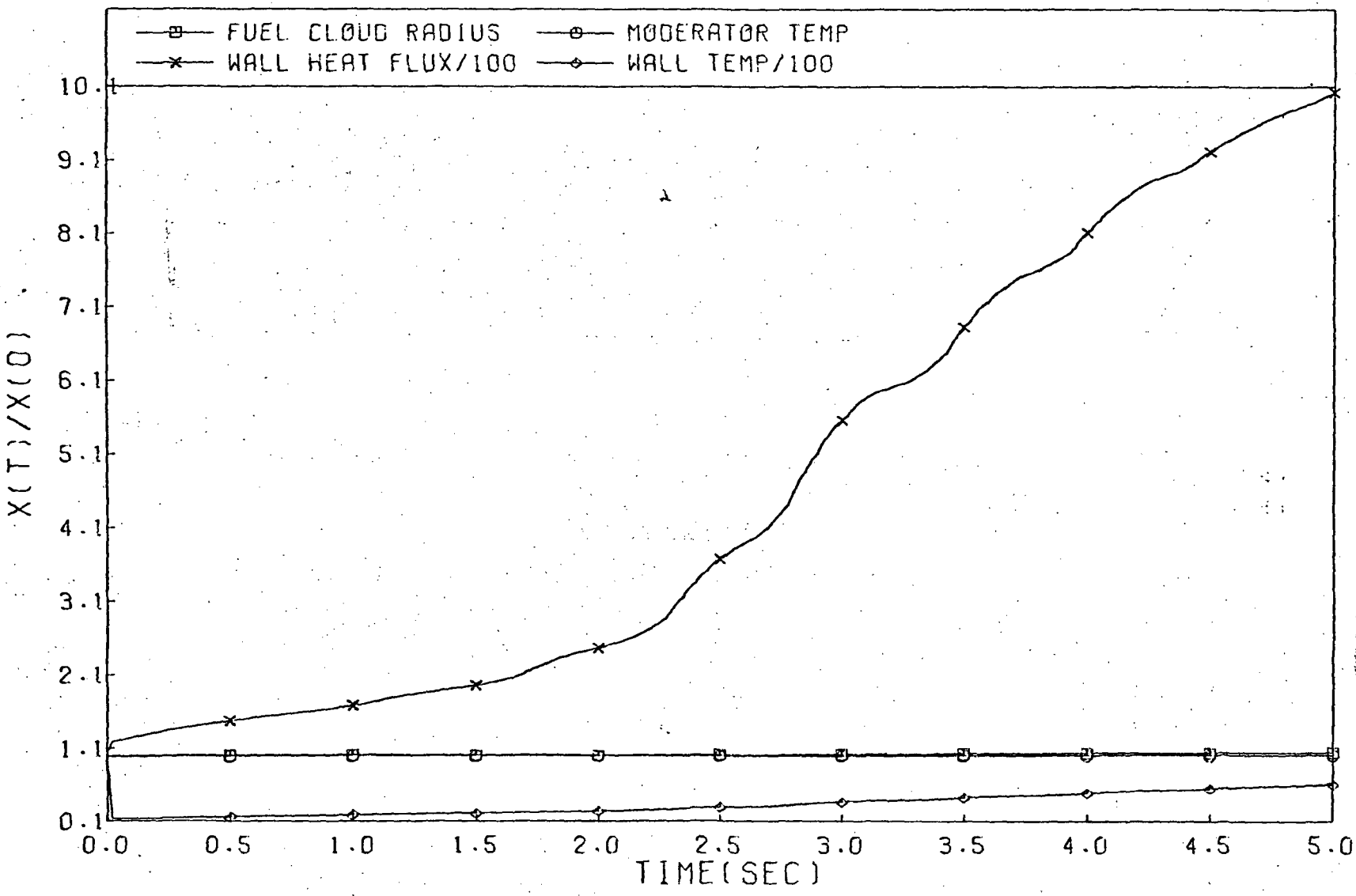

Figure 5-4. Response for a 20% Decrease in Propellant Injection Rate

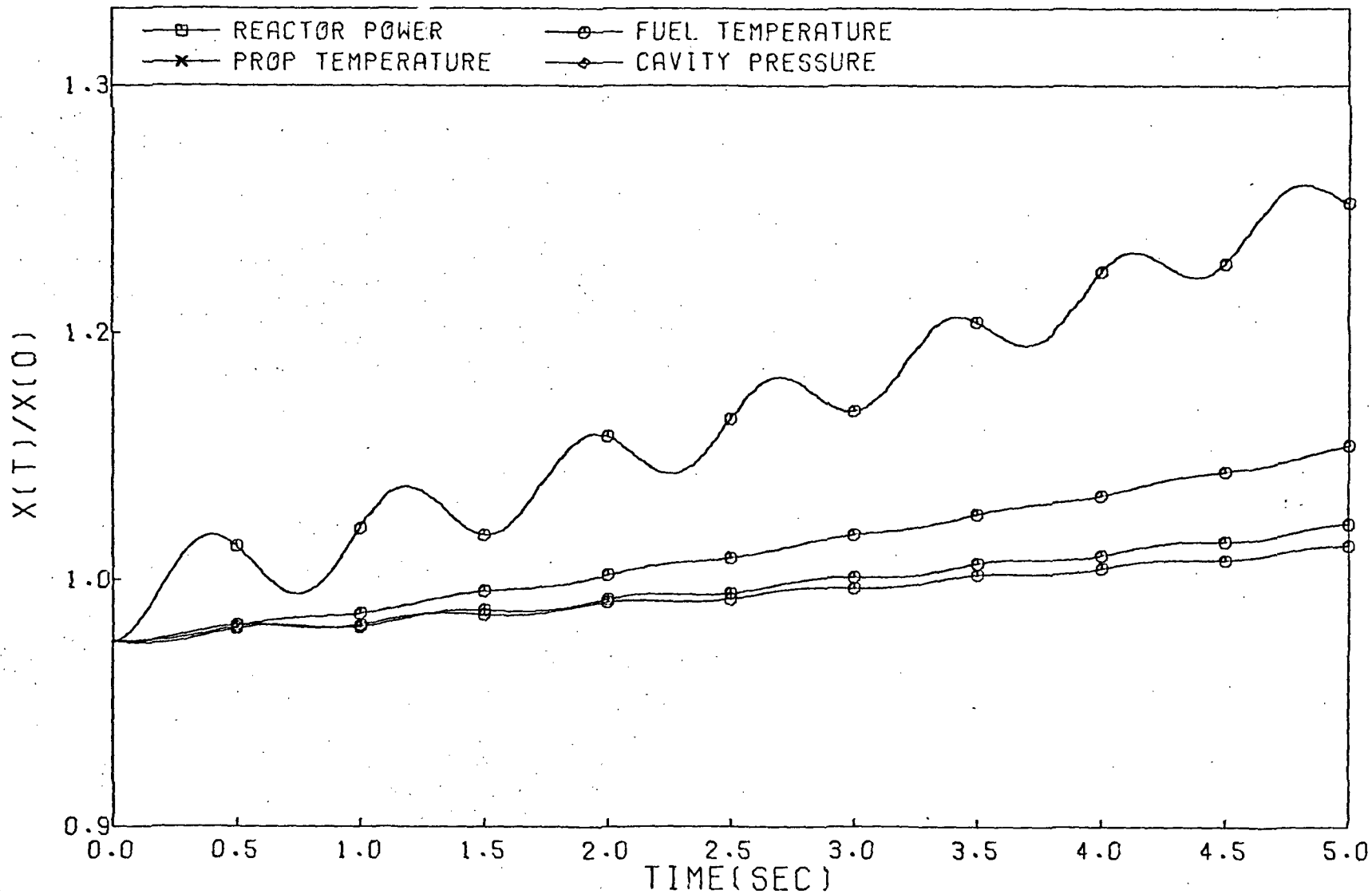

Figure 5-5. Response for a 5% Decrease in Propellant Injection Rate

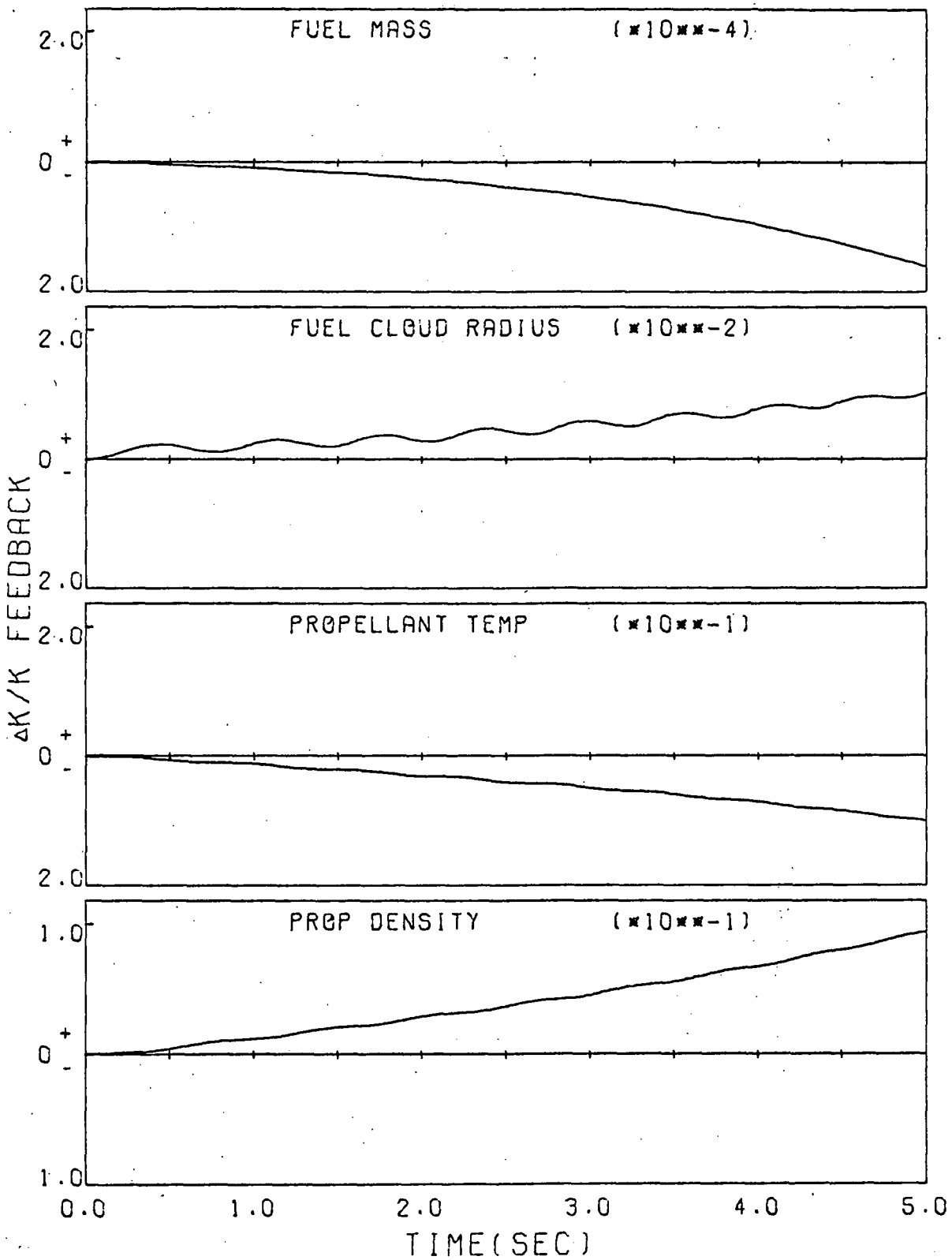

Figure 5-6. Components of Feedback Reactivity Following a 20% Decrease in Propellant Injection Rate

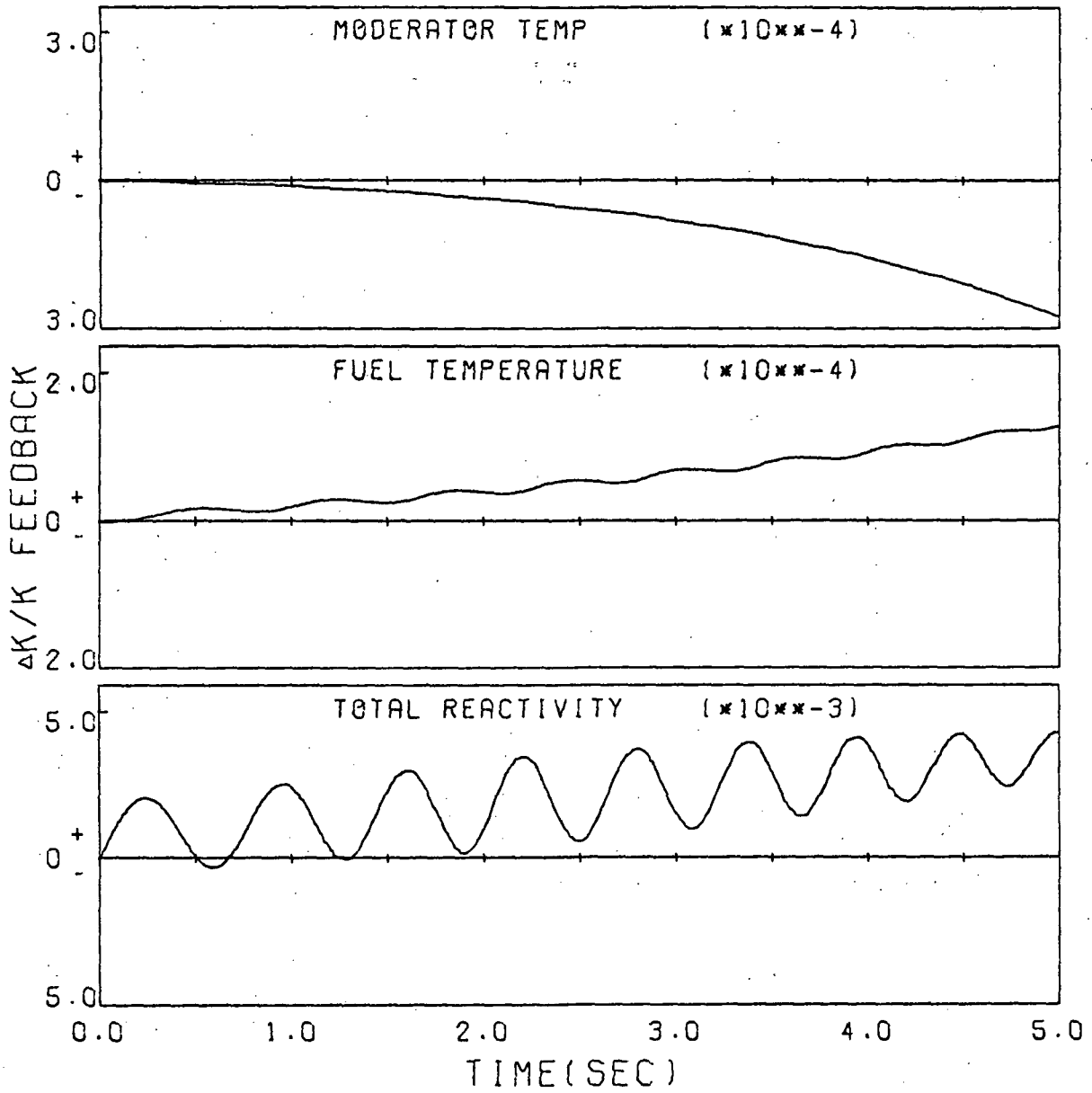

Figure 5-6. (cont.) Components of Feedback Reactivity Following a 20% Decrease in Propellant Injection Rate

appreciably to the overall response.

The effect on the system of increasing the propellant injection rate by 20% is shown in Figure 5-7. Unlike the response to a step insertion of negative reactivity, the power never rises to steady state levels after the injection rate increase; the highest power level after the perturbation is 13% below the design level. Sixty per cent of design power is reached after five seconds.

The reactivity plots of Figure 5-8 show that increases in propellant injection rate simply produce effects opposite those of injection rate interruptions, i.e., the propellant density increases and the fuel cloud shrinks yielding enough negative reactivity to offset the positive effect of the falling propellant temperature.

Examination of Figures 5-9 and 5-10 indicate that the increase by 20% of the fuel injection rate has an almost negligble effect on the state of the reactor. This conclusion can be drawn for all perturbations of the fuel injection rate. The reason for this inability to produce change is simply that the fuel injection rate is so small with respect to the contained fuel mass that even large percentage changes in the injection rate take expremely long times to significantly alter the fuel mass contained.

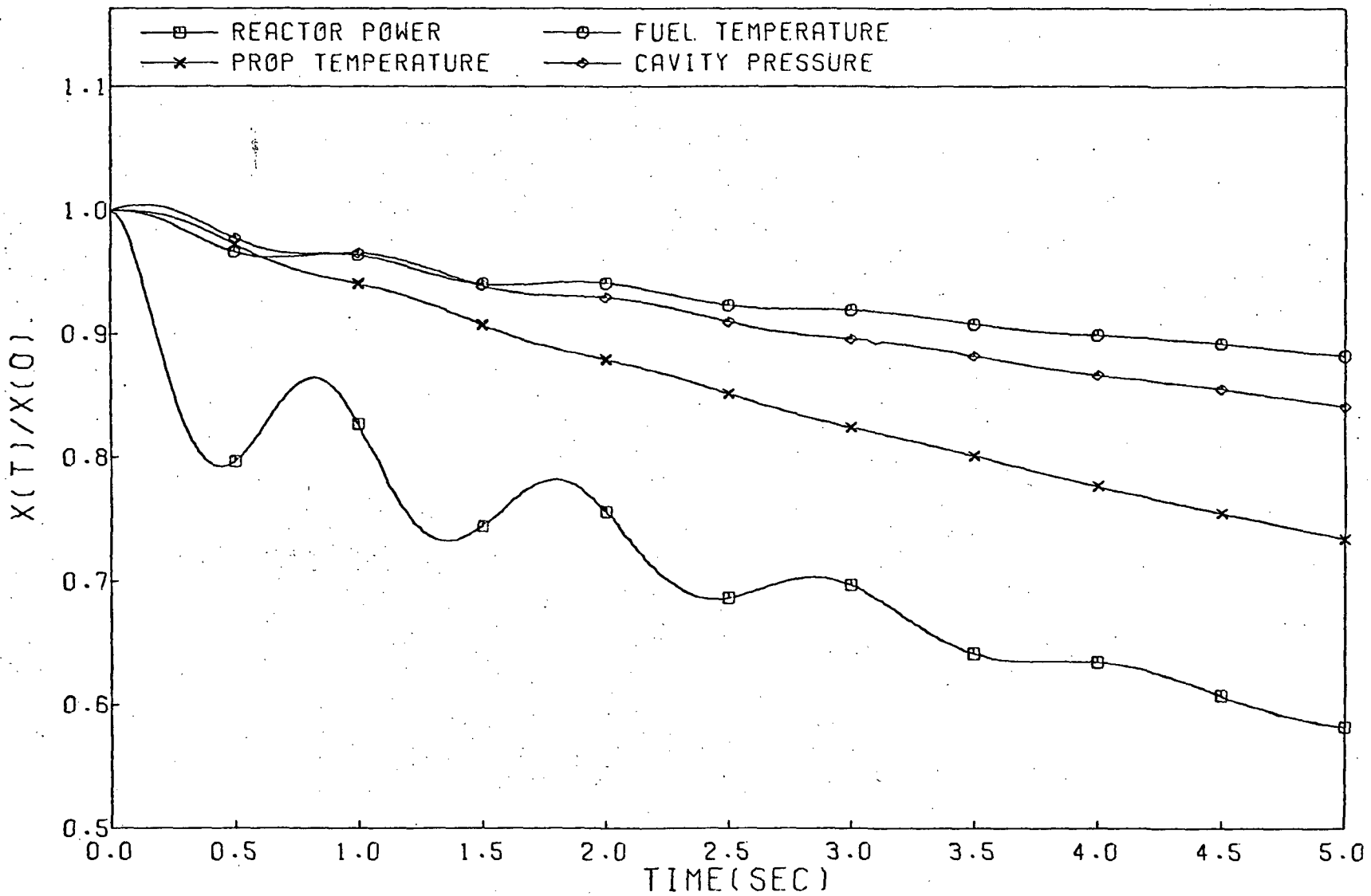

Figure 5-7. Response for a 20% Increase in Propellant Injection Rate

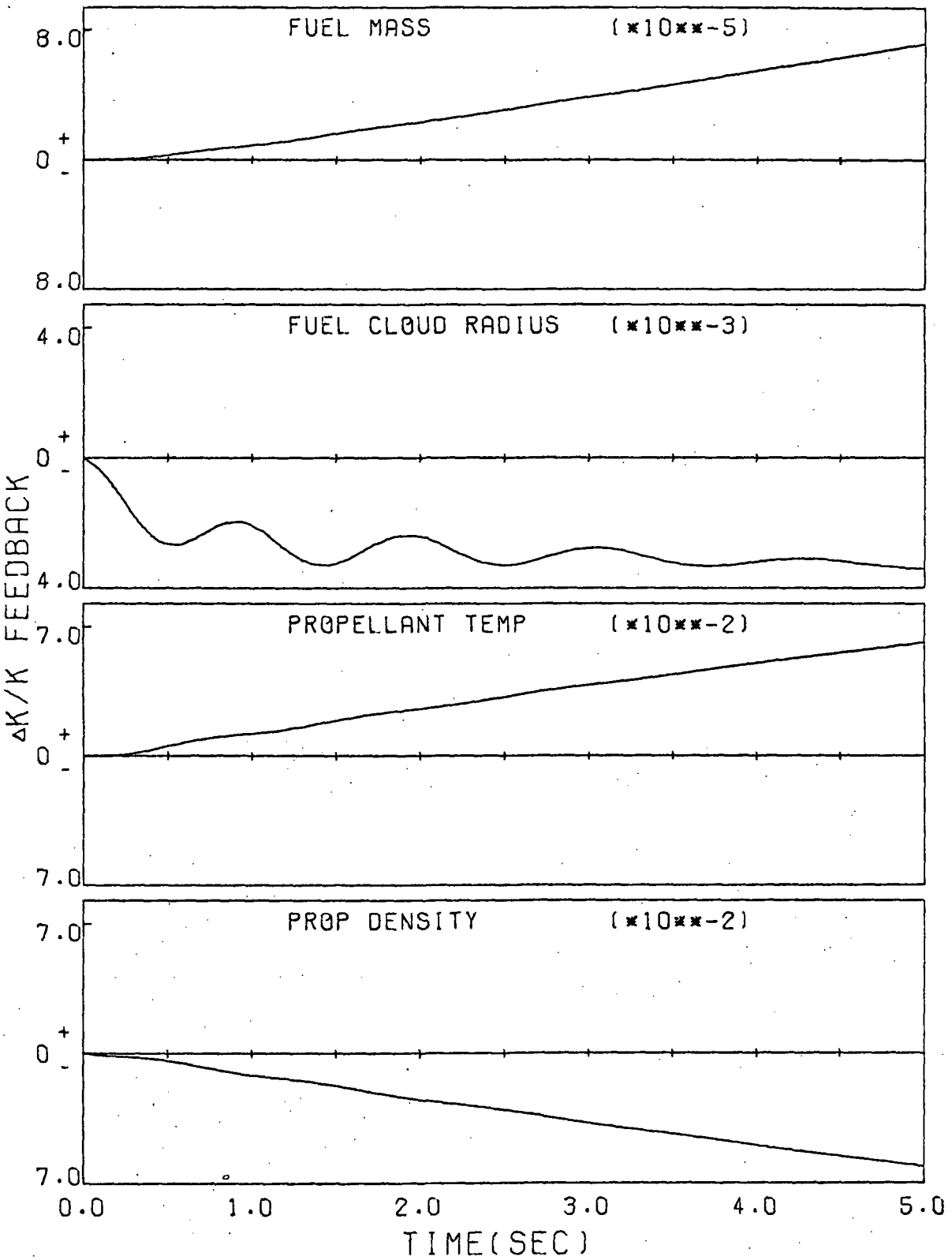

Figure 5-8. Components of Feedback Reactivity Following a 20% Increase in Propellant Injection Rate

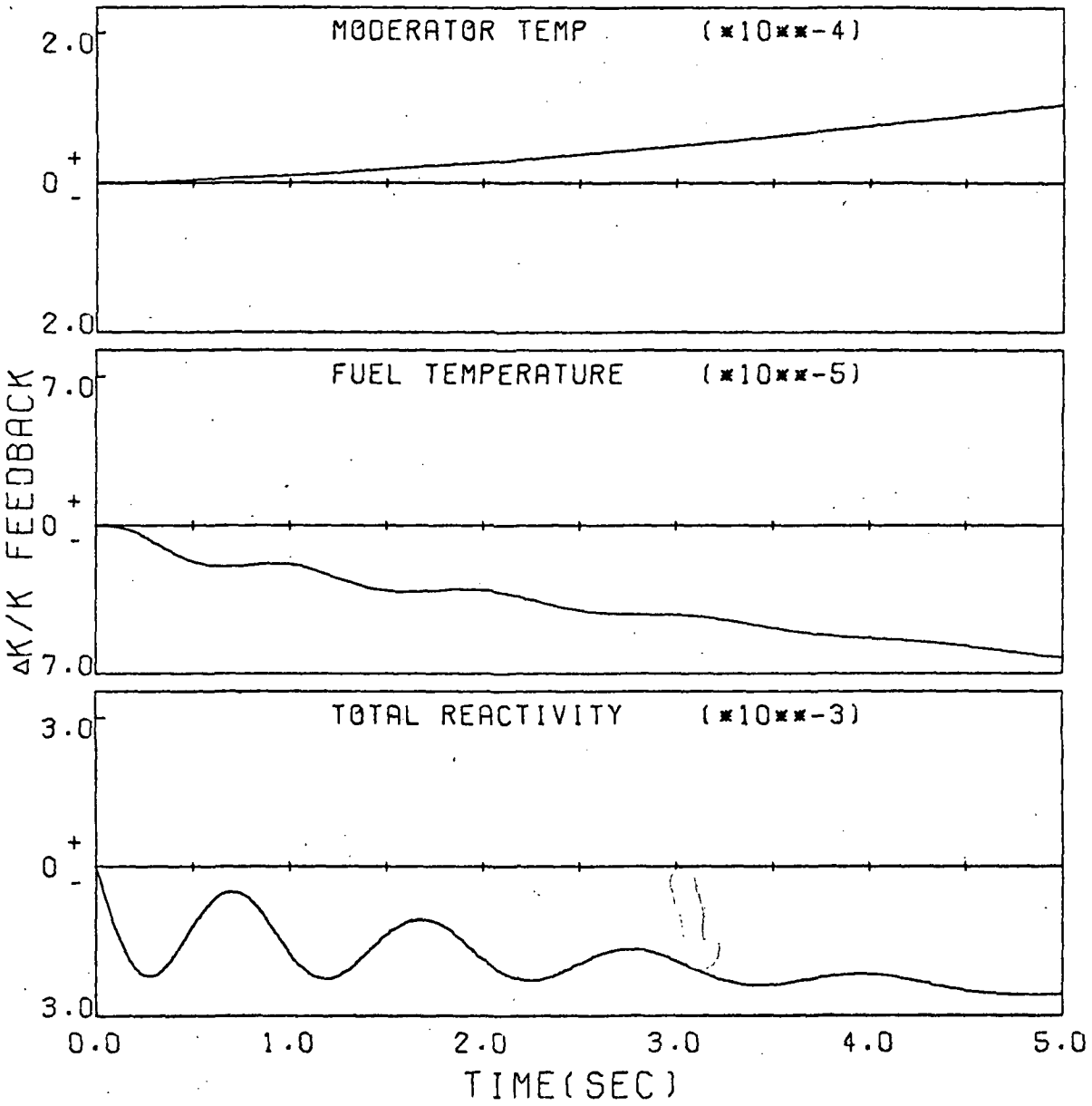

Figure 5-8. (cont.) Components of Feedback Reactivity Following a 20% Increase in Propellant Injection Rate

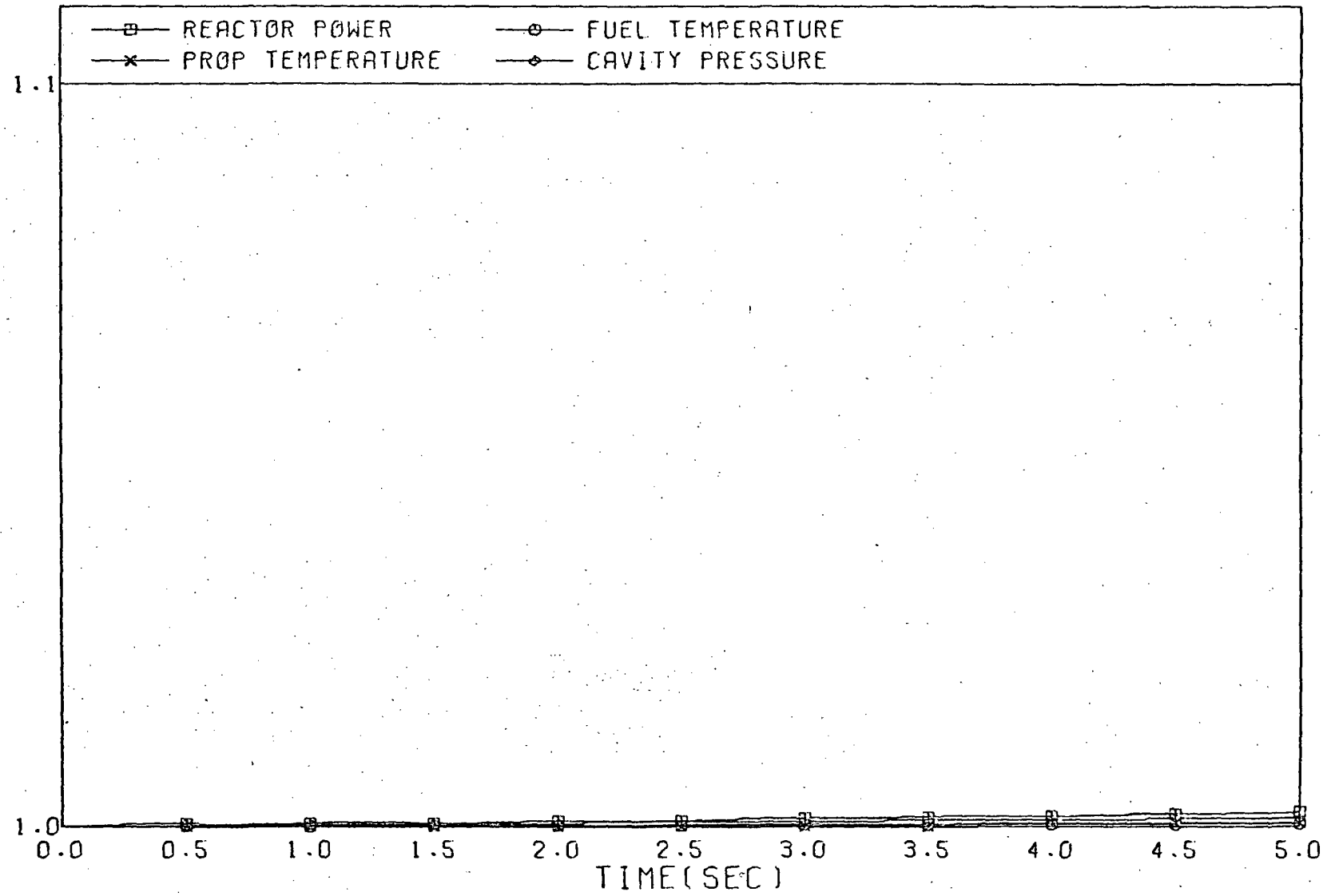

Figure 5-9. Response for a 20% Increase in Fuel Injection Rate

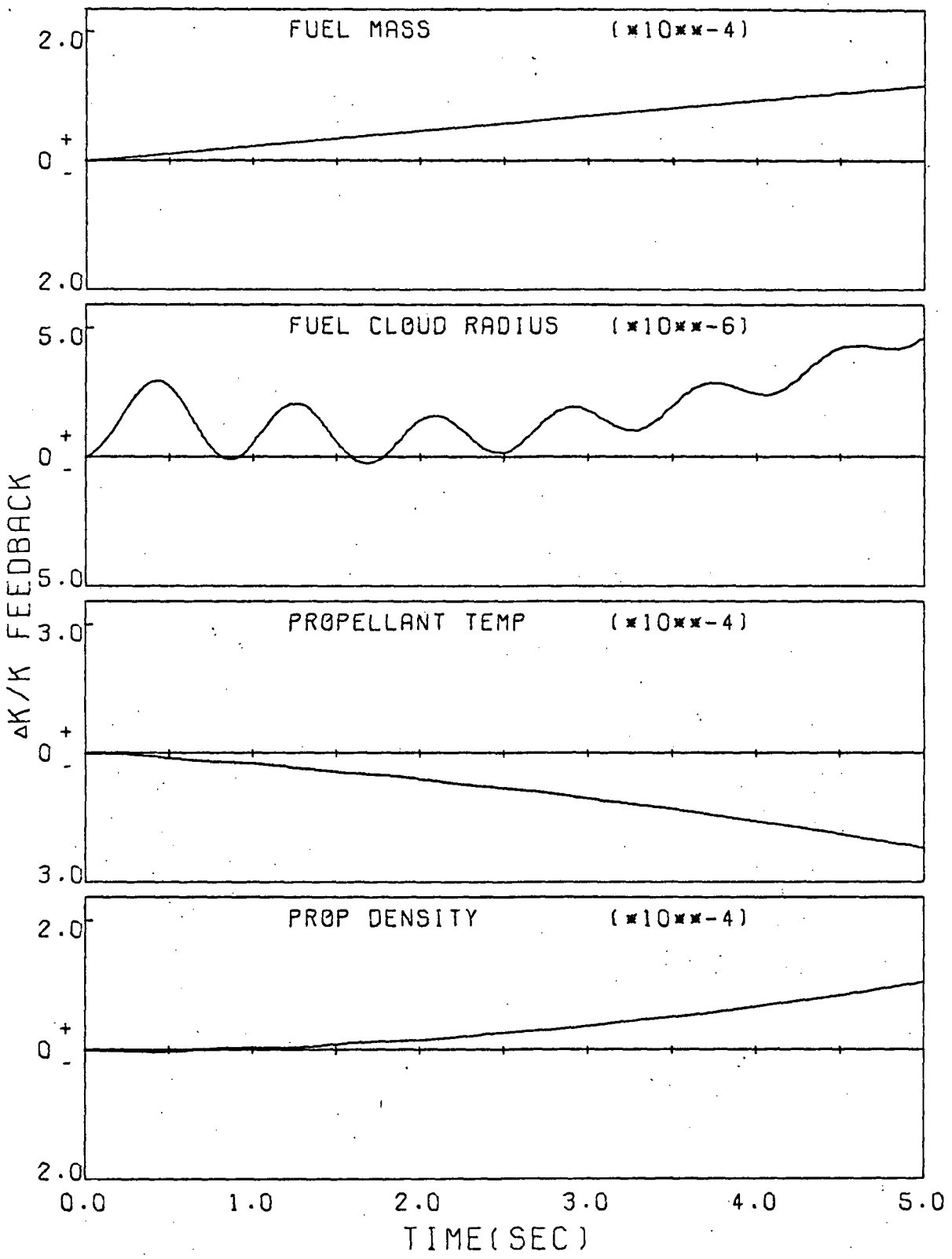

Figure 5-10. Components of Feedback Reactivity Following a 20% Increase in Fuel Injection Rate

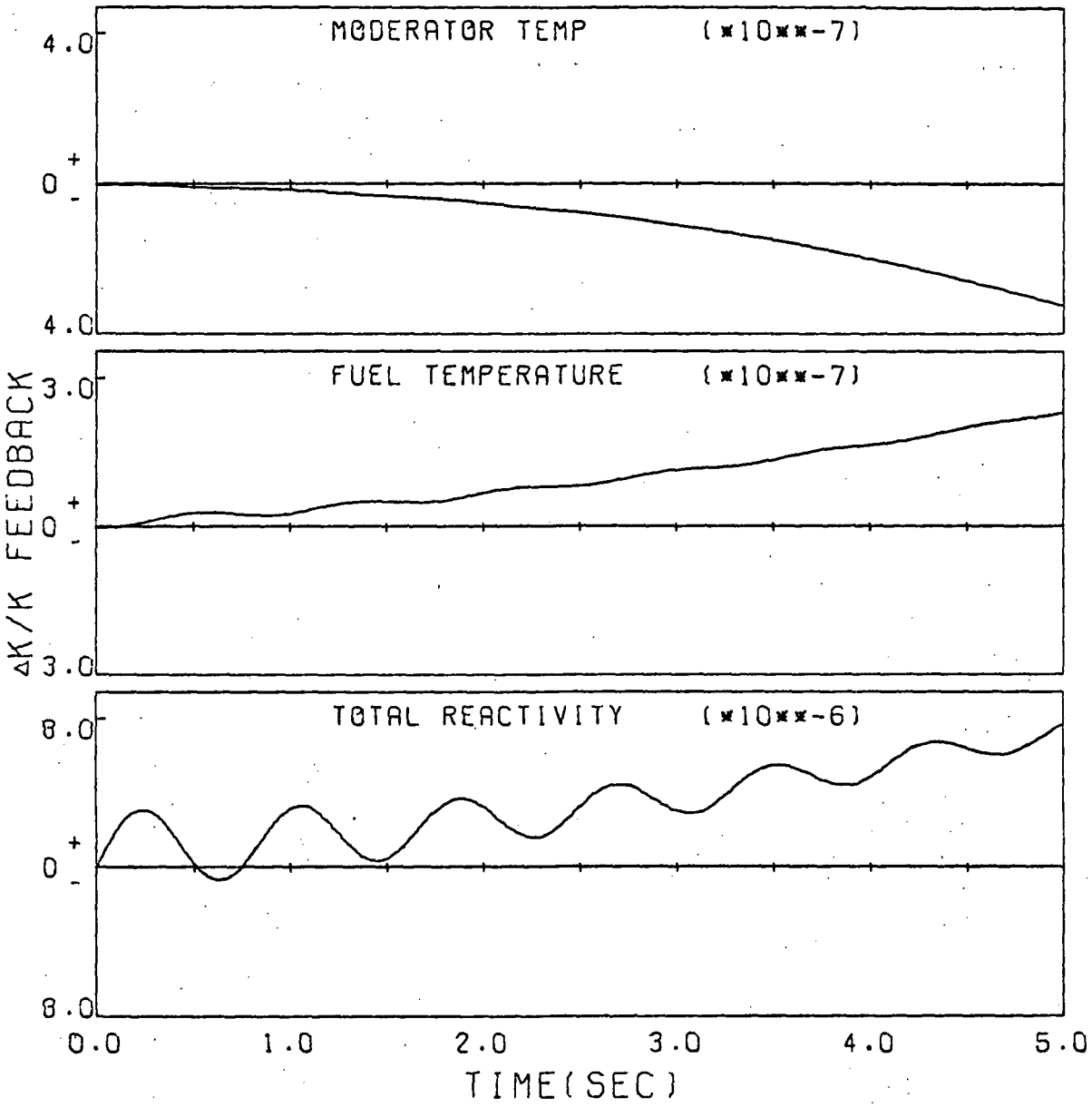

Figure 5-10. (cont.) Components of Feedback Reactivity Following a 20% Increase in Fuel Injection Rate.

Section 6

THE RESPONSE OF THE CONTROLLED REACTOR

The primary goal of this task was to determine the response characteristics of the controlled reactor. Three types of control were investigated: control drums situated on the moderator which would be capable of inserting negative reactivity, control of the rate of propellant injection, and control of the rate of fuel injection. The monitored parameters (whose value changes triggered the control systems) were taken to be reactor power, propellant temperature, and cavity pressure. Loop closures with each monitored parameter coupled to each control method were investigated. For each loop closure, delay times (attributable to sensing delays and the inertia of control system components) of .1, .5 and 2.0 seconds were investigated; a total of 27 control configurations were to be investigated.

Mathematically, the control schemes were modeled in the following way. If x is the monitored parameter (reactor power, propellant temperature or cavity pressure) and y is the controlled parameter (reactivity, propellant injection rate, or fuel injection rate), the differential equation for parameter y was modified to take the form

$$\frac{dy}{dt} = \left(\frac{dy}{dt}\right)_r + \left(\frac{dy}{dt}\right)_c \qquad (6\text{-}1)$$

where the first term on the right of the equation is the expression given for the time rate of change of y in Reference 16, and the second term is given by

$$\left(\frac{dy}{dt}\right)_c = C_{prop}\, y_{max}\, ((x(t-\tau) - x_o)/\, x_o) \qquad (6\text{-}2)$$

C_{prop} is a constant of proportionality which determines the degree to which a given change in the monitored parameter changes the value of the controlled parameter; the larger the value of C_{prop}, the more

dramatic the effect of a given change in x. The constant y_{max} is unity for y's other than reactivity. For cases in which reactivity was being controlled, y_{max} was the maximum reactivity insertable through the use of the control drums. τ is simply the loop time-delay in seconds. Negative values for the injection rates were not allowed; in cases in which a negative value was computed, the injection rate was set equal to zero. The value of C_{prop} was adjusted parametrically to insure that unreasonably high flow rates were not attained during the controlled response period.

The perturbation for all controlled responses was a positive insertion of .65% reactivity.

Reactivity Control

Figure 6-1 is a plot of the reactor response using reactor power as the monitored parameter, reactivity as the controlled parameter and 0.1 seconds as the loop time-delay. As is easily seen, the response takes the form a divergent oscillations making the reactor response less stable than with no control mechanism. The reason for the control system accomplishing exactly the opposite result as that desired is that the loop time-delay is of the same order of magnitude as the characteristic oscillation period of the reactor. The control system first "sees" the deviation from steady state at 0.1 second after the insertion; at this time, the power is still rising, but negative reactivity feedback mechanisms are beginning to become significant. The control mechanism initially inserts negative control reactivity, which is correct, but negative control reactivity is inserted even after the power level drops below the steady state value. This is, of course, because the control system is still responding to the power as measured 0.1 second earlier. The more rapid drop in the power level causes the reactor to exhibit asymmetric behavior as described in Section 4. The tendency toward larger and larger oscillations is enhanced by the fact that as the power passes the steady state level, the control system adds reactivity for 0.1 second that drives the reactor farther from steady state.

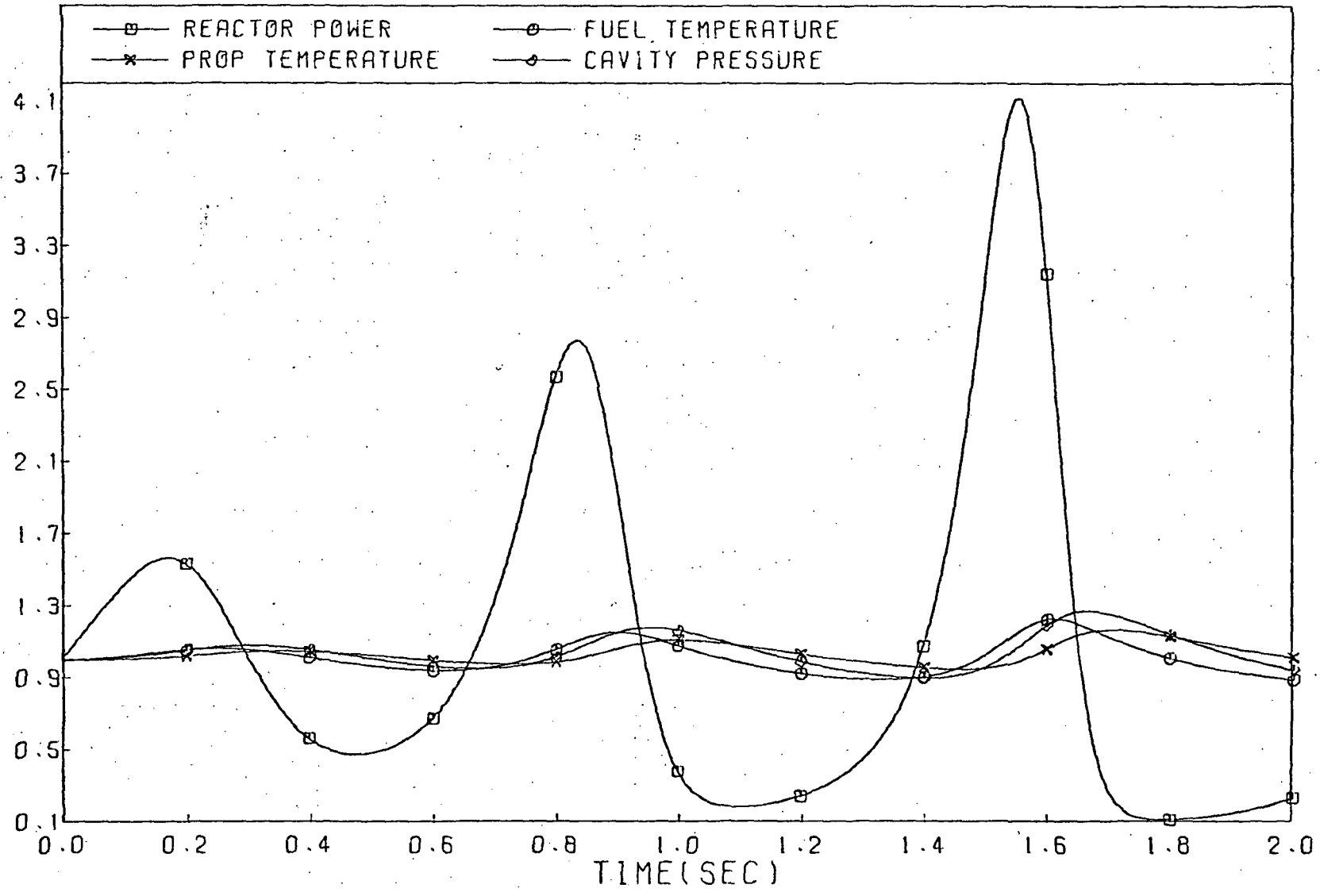

Figure 6-1. Response using Reactor Power as the Monitored Parameter, Reactivity as the Controlled Parameter and a Loop Time-Delay of .1 seconds

An increase of the loop time-delay constant to 0.5 seconds produced the result shown in Figure 6-2. Like the response described above, the oscillations of the power response are divergent; again, the mechanism producing the instability is the introduction of reactivity based on the initial power response when the action required to control the reactor at the time of the introduction is quite different.

The results obtained using the same loop closure and a loop time-delay of 2.0 seconds is shown in Figure 6-3. In this case, the problem of controlling a system whose characteristic response is oscillatory is even more pronounced. At two seconds after the insertion, the power is below its steady state value, but negative reactivity is inserted because the power on which the control system is acting is above design level. The result of the insertion of the wrong reactivity value is again an unstable oscillation in reactor power.

Runs were made using reactivity as the controlled parameter and propellant temperature and cavity pressure as the measured parameters. Loop time-delay constants of 0.1, 0.5 and 2.0 seconds were investigated for each loop closure. In each case, the response was almost identical to the results obtained in the corresponding case with reactor power as the measured parameter. This result was not surprising since both propellant temperature and cavity pressure oscillate with the reactor power.

Since succesful control of the reactor was not obtained using the specified time delays, a parametric study was undertaken to find the maximim delay for which the control system could bring the power back to steady state. It was found that a loop time-delay of .002 seconds was the largest for which the response became stable. The response obtained using this delay is shown in Figure 6-4.

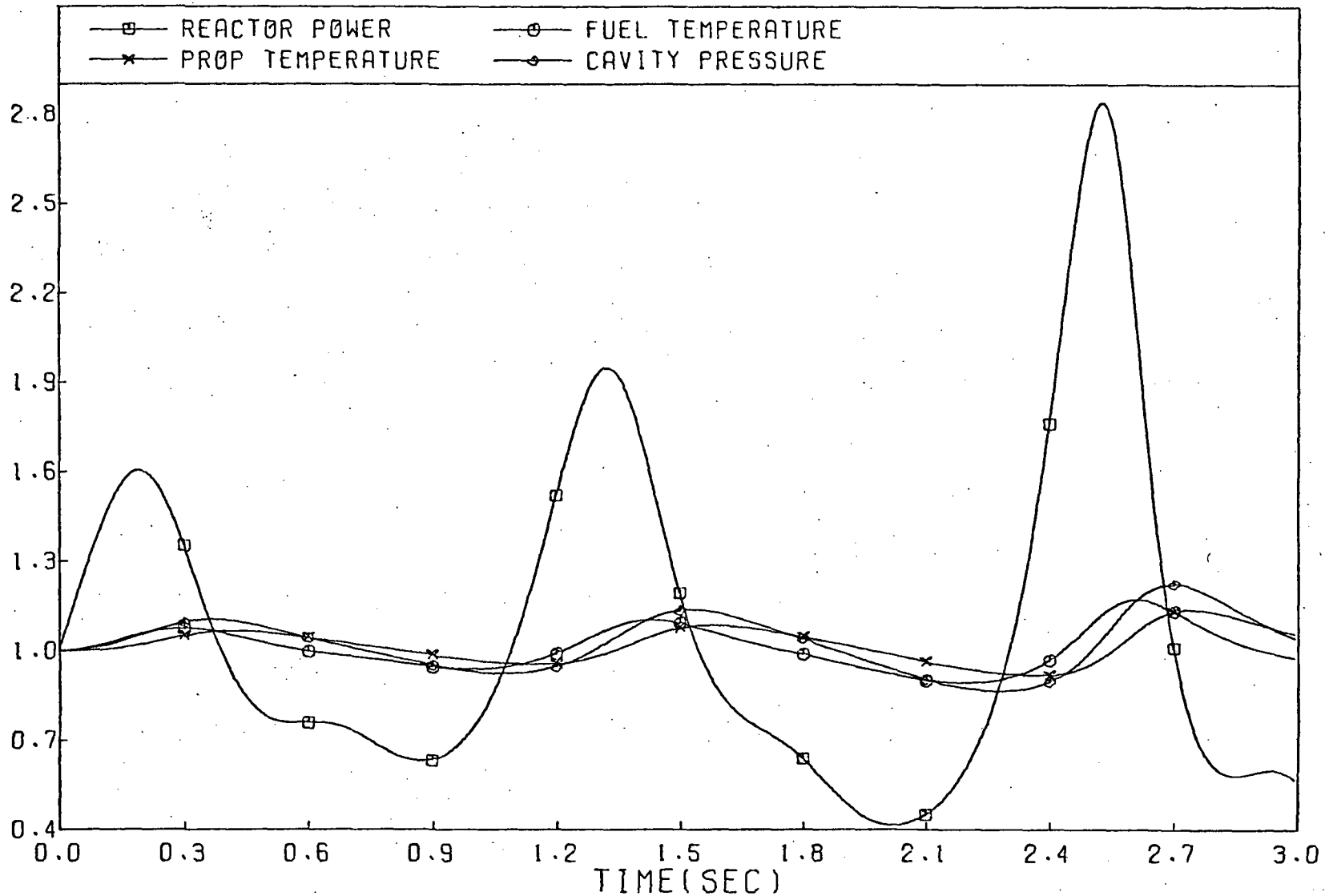

Figure 6-2. Response using Reactor Power as the Monitored Parameter, Reactivity as the Controlled Parameter and a Loop Time-Delay of .5 seconds

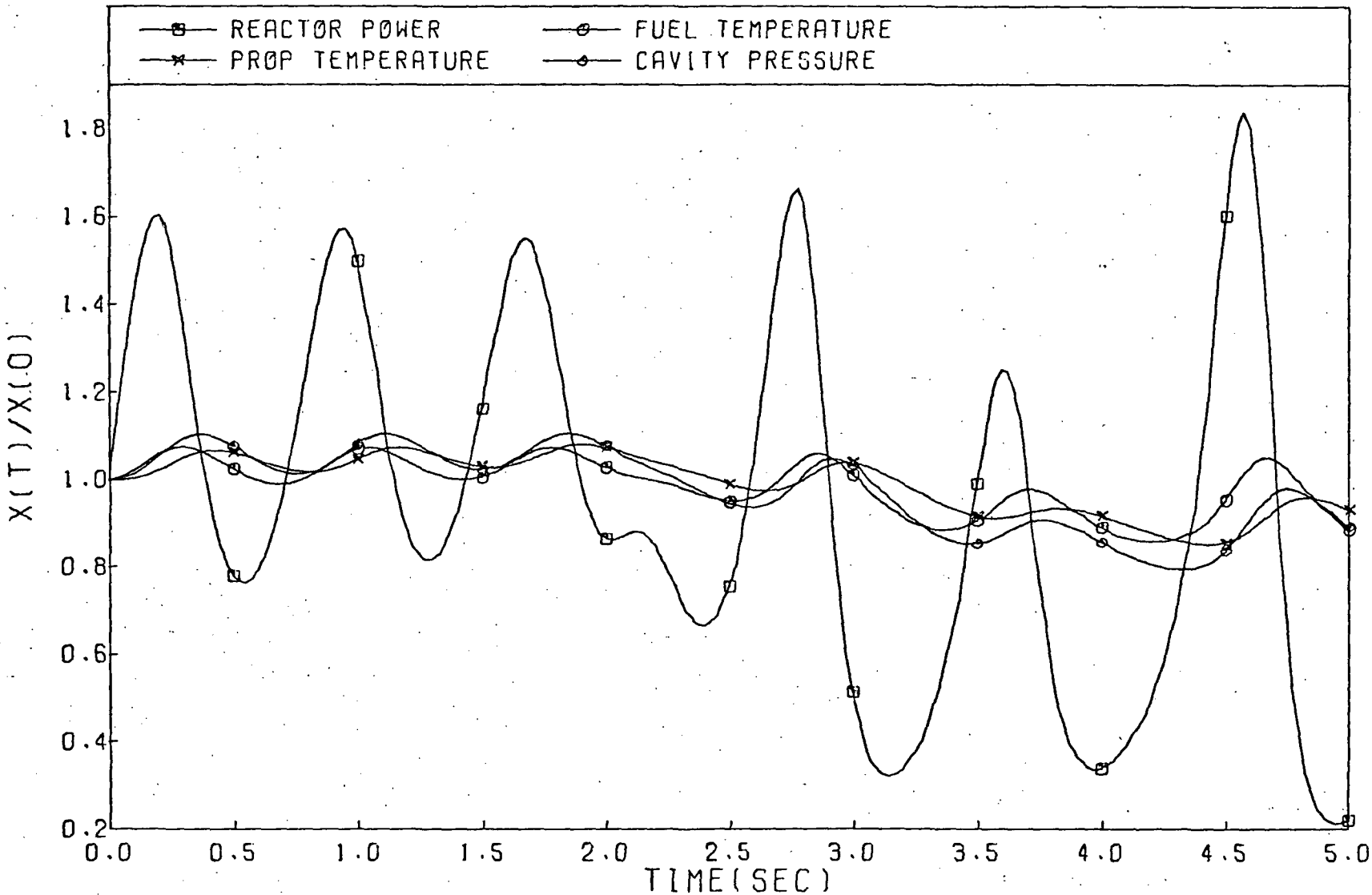

Figure 6-3. Response using Reactor Power as the Monitored Parameter, Reactivity as the Controlled Parameter and a Loop Time-Delay of 2.0 seconds

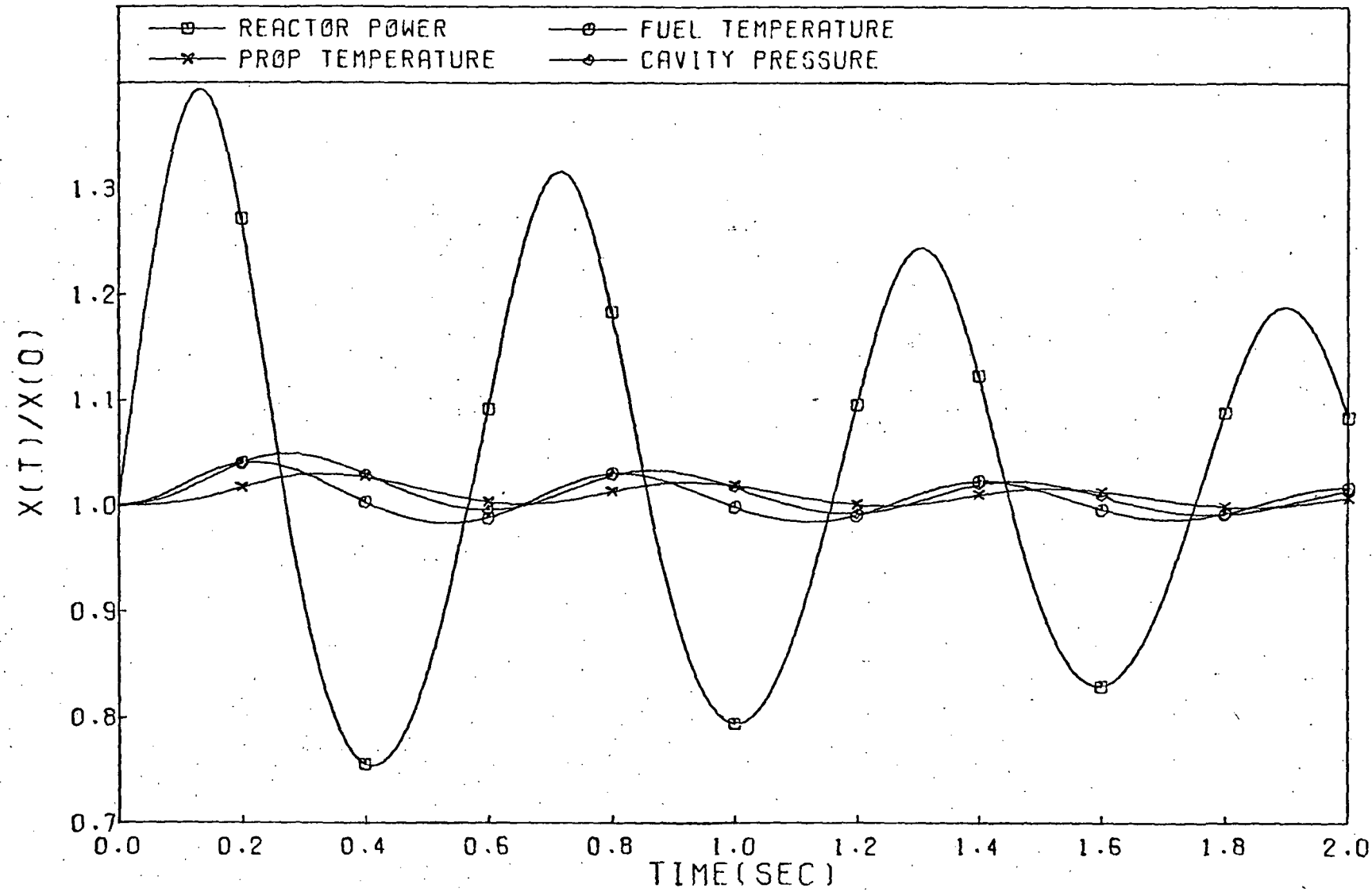

Figure 6-4. Response using Reactor Power as the Monitored Parameter, Reactivity as the Controlled Parameter and a Loop Time-Delay of .002 seconds

Propellant Injection Control

As can be seen readly from Figure 6-5, the qualitative results using propellant injection as the controlled parameter and reactor power as the monitored parameter with a loop time-delay of 0.1 seconds are essentially the same as those in the corresponding case described above, i.e., the power begins to oscillate unstably. The reasons for this behavior are also basically the same. The propellant injection rate is increased (negative reactivity effect) when the power level is already moving in a negative direction and decreased (positive reactivity effect) when the power level is rising. The net effect is, of course, that the power is driven farther from its design point at each oscillation.

Similarly disastrous results are obtained when the loop time-delay is increased to 0.5 seconds; the calculated response is shown in Figure 6-6. Again, the initial control reaction is an increase in propellant injection based on the power increase occuring near $t = 0$. However, at the time of the control injection increase (0.5 seconds), the reactor power is already below design level and the control drives it to still lower levels, thus leading to an unstable response.

The response obtained using reactor power as the monitored parameter and propellant injection as the controlled parameter with a loop time-delay of 2.0 seconds is shown in Figure 6-7. Qualitatively, the response is identical to that of Figure 6-6, but the time delay between the initial control action and the first power excursion is correspondingly longer.

With one notable exception, all of the runs using propellant temperature or cavity pressure as the monitored parameter and propellant injection as the controlled parameter produced results identical to those using reactor power as the monitored parameter. As can be seen from the response depicted in Figure 6-8, using the propellant temperature-propellant injection control loop with a time delay of

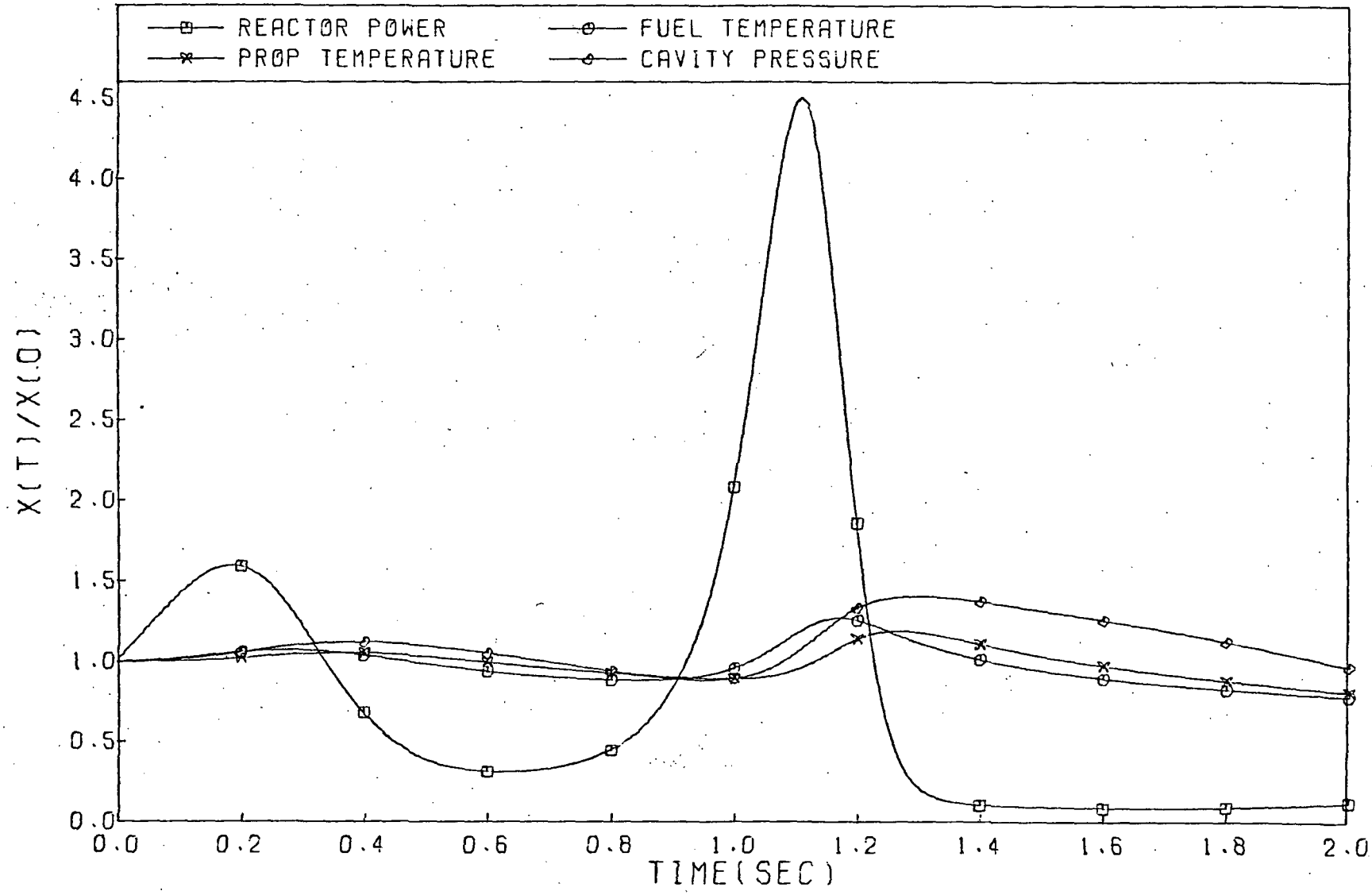

Figure 6-5. Response using Reactor Power as the Monitored Parameter, Propellant Injection as the Controlled Parameter and a Loop Time-Delay of .1 seconds

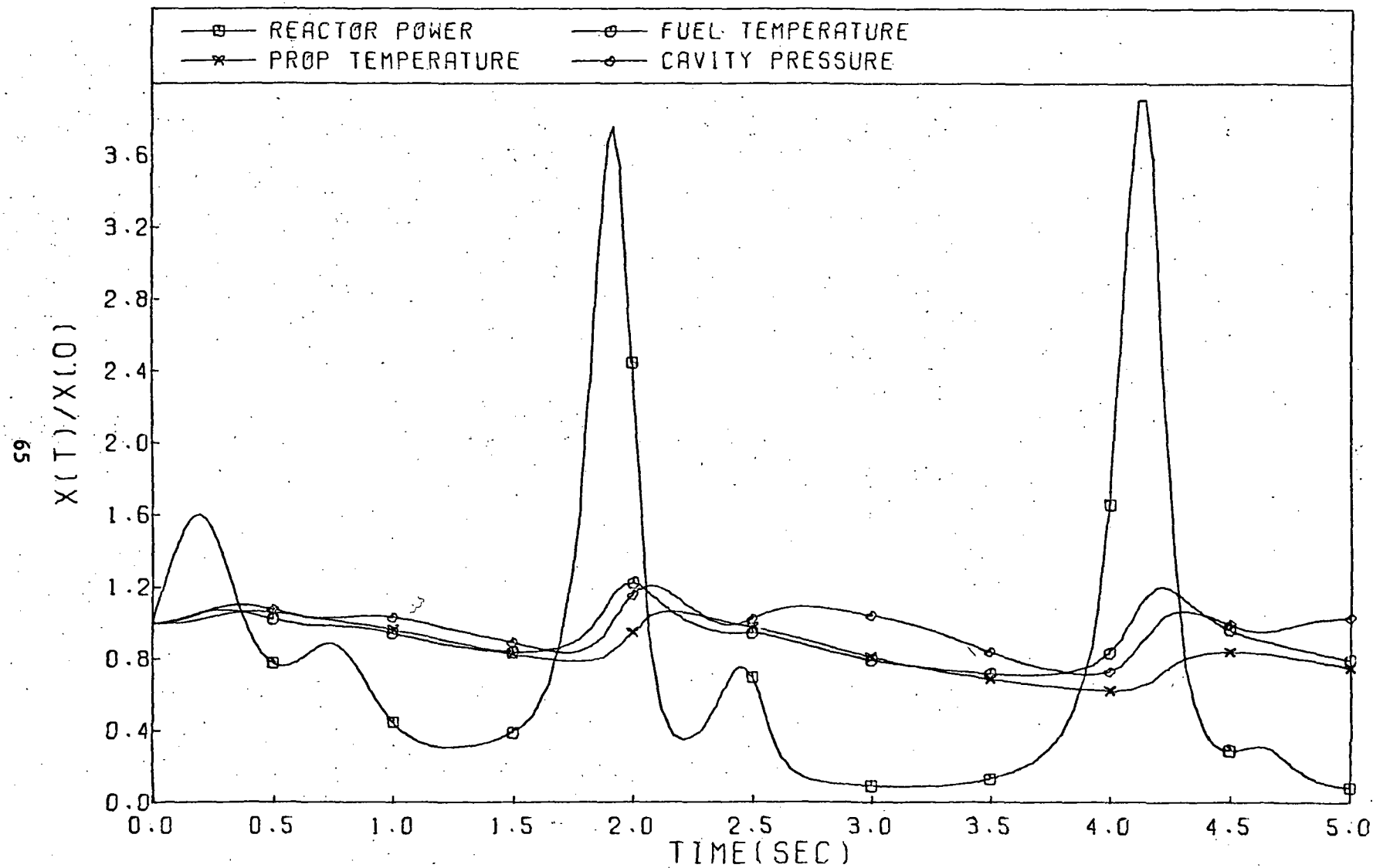

Figure 6-6. Response using Reactor Power as the Monitored Parameter, Propellant Injection as the Controlled Parameter and a Loop Time-Delay of 2.0 seconds.

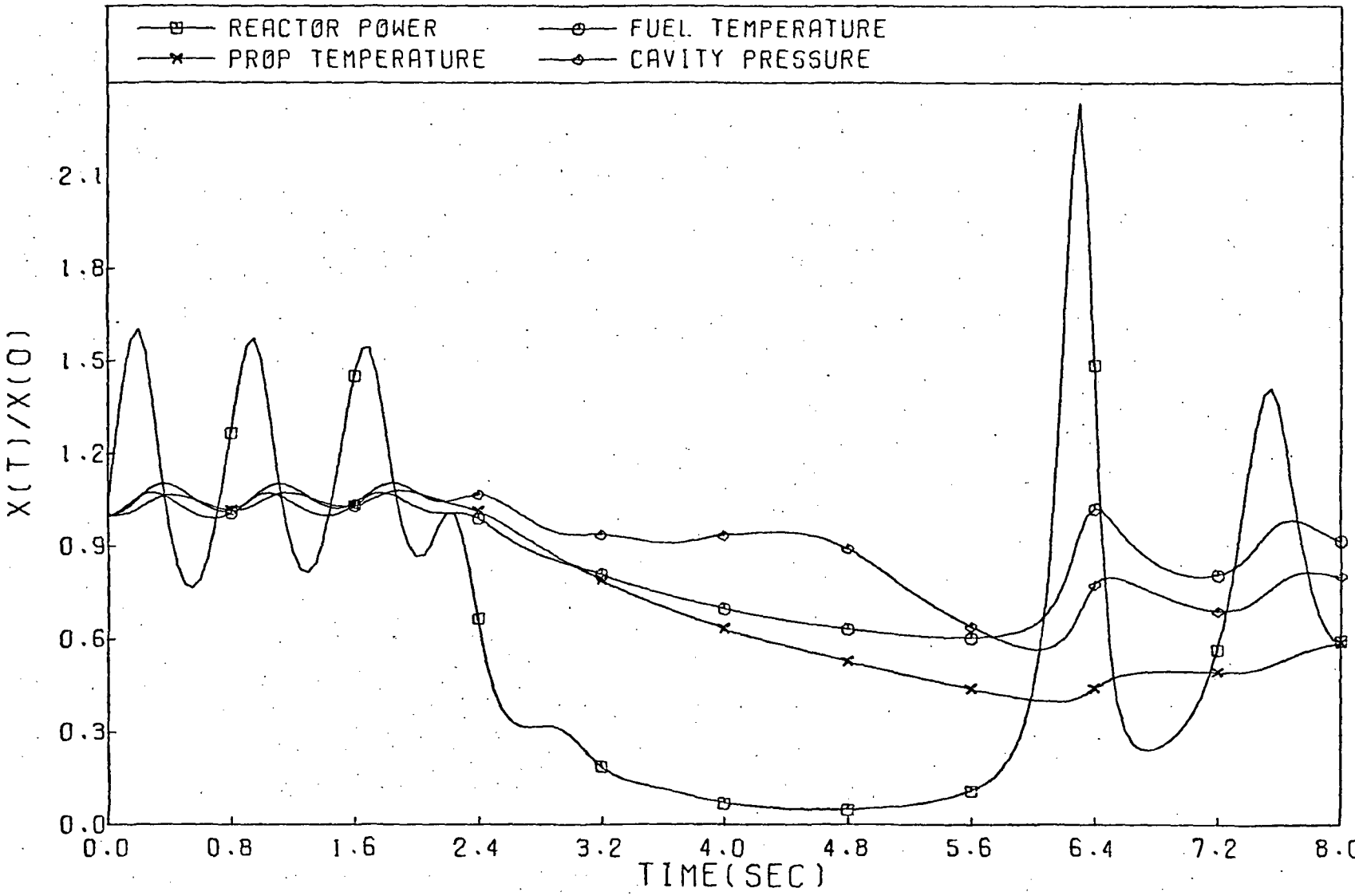

Figure 6-7. Response using Reactor Power as the Monitored Parameter, Propellant Injection as the Controlled Parameter and a Loop Time-Delay of 2.0 seconds.

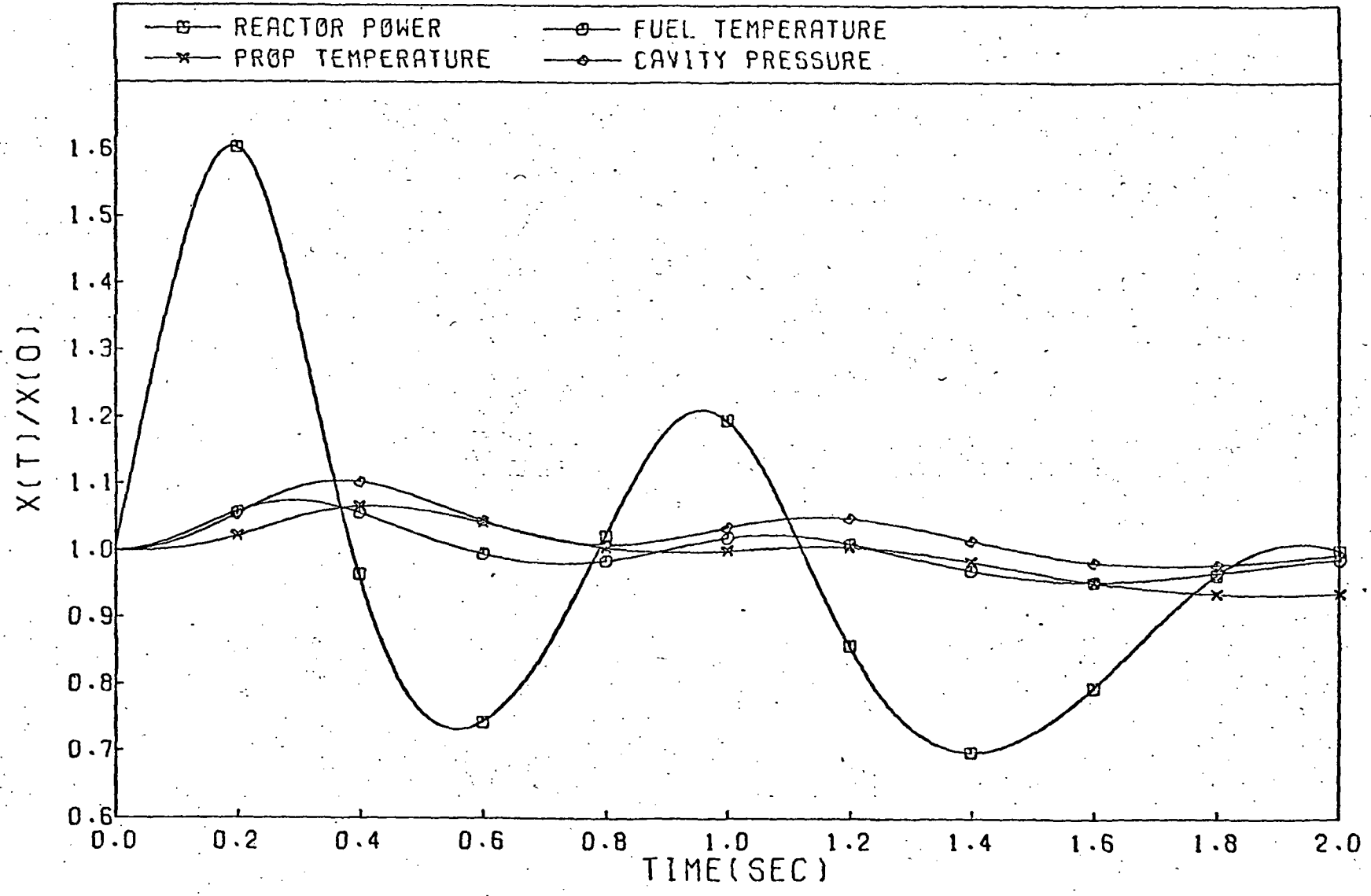

Figure 6-8. Response using Propellant Temperature as the Monitored Parameter, Propellant Injection as the Controlled Parameter and a Loop Time-Delay of .1 seconds

0.1 seconds gives a totally different response picture. The difference is due to an additional feedback loop inherent in the equation governing the behavior of the propellant temperature. Increases in the propellant temperature causes the injection rate to increase and the contained propellant mass to rise. The rise in propellant mass tends to make the response of the propellant temperature more sluggish. Of course, the opposite is true of situations in which the propellant temperature is falling. The result of adding this additional feedback loop causes the power to oscillate around a slowly falling average power. The propellant mass-propellant temperature interaction does not occur when longer delay times are used, and, hence, reactor behavior is not affected.

As was shown in Section 5, decreases in propellant injection rate cause very rapid increases in the cavity wall heat flux. In all of the automatic control responses discussed using propellant injection control, the injection rate called for by reactor behavior dropped below the value required to keep the cavity wall heat flux below burnout. As the power dropped below steady state the propellant injection rate was decreased to introduce positive reactivity, but the wall heat flux exceeded burnout values due to the arrested inlet flow. For this reason, it was concluded that regulation of the propellant injection should not be considered further as the control parameter in automatic control loops. Conditions leading to disastrous reductions in propellant flow will inevitably result if automatic systems are given exclusive control of the feedback loop. The powerful negative reactivity effect associated with increases in the injection rate could safely be used for operations such as shutting down the reactor.

Fuel Injection Control

As will be remembered from the discussion of the effect on the reactor of changing the fuel injection rate, the rate of introduction of fuel at or near steady state values has very little effect on the

state of the reactor. Also, preliminary studies reported in Reference 16 indicated that regulation of the fuel injection rate was inadequate for all but the smallest perturbations. Based on the above mentioned previous information, it was suspected that fuel injection control would not be of interest in controlling the response of perturbations of interest.

In order to determine if fuel injection regulation is a viable control alternative, one run was made with the standard perturbation of .65% reactivity inserted simultaneously with a complete shutoff of fuel injection. The predicted response was virtually identical to that observed with no control mechanisms. Since this case represents an overestimation of the realizable effect of fuel injection control methods, it was concluded that the control of the rate at which fuel is introduced into the reactor cavity is not an adequate control method for the reactor. No further runs to investigate fuel injection control were made.

Control of Other Perturbations

Although a positive reactivity insertion of .65% was the perturbation used to evaluate all the control methods mentioned above, control of other disturbances warrants some discussion. As is probably well remembered, even large percentage changes in the fuel injection rate do not noticibly affect the state of the reactor; any control system which is suitable for controlling reactivity insertions will be more than adequate to control changes due to variations in the fuel injection rate. As was depicted graphically in Figure 3-6, however, reductions in the propellant injection rate produce rapid rises in reactor power and instantaneous wall burnout.

Since the burnout of the cavity wall occurs immediately as the propellant flow is cut off, no control system can possibly react rapidly enough to prevent wall damage. Burnout due to this mech-

anism must be avoided through judicious reactor design; either the steady state wall heat flux must be even farther below the wall burnout value or the hydrogen pumping system must be designed so that interruptions in the propellant injection rate cannot occur. Implicit in the latter method is the implication that regulation of propellant inlet flow cannot be used as a control mechanism.

Section 7

CONCLUSIONS

Conclusions which were drawn from the research presented in this report are as follows.

1. The model described herein is sensitive to moderate variations in the propellant temperature, propellant density and fuel cloud expansion coefficients of reactivity and large changes in the fuel temperature reactivity coefficient.

2. Increases in wall heat flux due to increased fuel-propellant heat transfer following positive reactivity insertions does not present a control problem which could not be solved with state-of-the-art control techniques.

3. Decreases in the propellant injection rate cause instantaneous wall burnout which can only be avoided through judicious reactor design; control systems cannot be made to react rapidly enough to prevent cavity wall damage.

4. Control methods using regulation of the fuel injection rate were found to be inadequate for controlling perturbations of interest.

5. Propellant injection control was found to be potentially dangerous when used with an automatic control system.

6. The use of control drums in the moderator region was found to be the best candidate for reactor control, although the delay time for direct linear control must be on the order of 10^{-3} seconds.

BIBLIOGRAPHY

1. Clement, J. D. and Williams, J. R., "Gas-Core Reactor Technology," Reactor Technology, 13, No. 1, 13-15 (July 1970)

2. Bussard, P. W. and DeLauer, R. D., Fundamentals of Nuclear Flight, McGraw-Hill, New York, 1965.

3. Ragsdale, R. G., Personal Communication, May 1970.

4. Rom, F. E., "Gaseous Nuclear Rocket," Patent No. 3,202,582, filed August 28, 1961.

5. Ragsdale, R. G., "Are Gas-Core Nuclear Rockets Attainable?" AIAA Paper No. 68-570, June 1968.

6. Ragsdale, R. G., "Relationship Between Engine Parameters and the Fuel Mass Contained in an Open-Cycle Gas-Core Reactor," NASA TM-X-52733, January 1970.

7. McLafferty, G. H., "Gaseous Reactor Container," Patent No. 3,223, 591, filed August 27, 1962.

8. McLafferty, G. H., "Investigation of Gaseous Nuclear Rocket Technology," Summary Technical Report, United Aircraft Research Laboratories Report No. H-9100093-46, November 1969.

9. Clark, J. W., Johnson, B. V., Kendall, J. L., Mansing, A. E., and Travers, A., "Open Cycle and Light-Bulb Types of Vortex-Stabilized Gaseius Nuclear Rockets," Journal of Spacecraft and Rockets, 5(8), 941 (August 1968).

10. Rosa, R. J., Magnetohydrodynamic Energy Conversion, McGraw-Hill, New York, 1968.

11. Sherman, A., "Gaseous Fission Closed Loop MHD Generator," Proceedings of the Symposium on Research on Uranium Plasmas and Their Technological Applications, University of Florida, January 1970.

12. Rosa, R. J., "Propulsion System Using a Cavity Reactor and Magnetohydrodynamic Generator," American Rocket Society Journal, July 1961.

13. Williams, J. R., and Shelton, S. V., "Gas Core Reactors for MHD Power Systems," Proceedings of the Symposium on Research on Uranium Plasmas and Their Technological Applications, University of Florida, January 1970.

BIBLIOGRAPHY (Continued)

14. Williams, J. R., Kallfelz, J. M., and Shelton, S. V., "A Parametric Survey of Gas-Core Reactor-MHD Power Plant Concepts," Proceedings of the Intersociety Energy Conversion Engineering Conference, Las Vegas, Nevada, September 1970.

15. Kallfelz, J. M. and Williams, J. R., "Exploratory Calculations for a Gaseous Core Fast Breeder Reactor," ANS Transactions 14, No. 1, November 1970.

16. Turner, K. H., Jr.,"A Dynamics Model of the Coaxial Flow Gaseous Core Nuclear Reactor System", Ph.D. Thesis, Georgia Institute of Technology, December 1971.